

Structural regularities in $2M_1$ dioctahedral micas: The structure modeling approach

BELLA B. ZVIAGINA* AND VICTOR A. DRITS

Geological Institute RAS, 7 Pyzhevsky per., 119017 Moscow, Russia

ABSTRACT

An improved algorithm has been elaborated for computing atomic coordinates in K-dioctahedral micas- $2M_1$ from the experimental data on cation composition and unit-cell parameters. The structure modeling procedure is based on regression equations relating the structural features and chemical composition of micas that were obtained from the analysis of published data on 27 refined structures of dioctahedral micas of various compositions including 20 K-dioctahedral micas- $2M_1$, 3 paragonites- $2M_1$, 2 margarites- $2M_1$, and 2 celadonites- $1M$. The empirical relationships accurately describe the observed structural distortions in dioctahedral micas, such as tetrahedral tilt and rotation, tetrahedral elongation, octahedral flattening, hydroxyl depression, etc. The majority of the regressions have $r^2 > 0.8$ and p-values < 0.05 , which means that the results are statistically significant. The predicted structural parameters are used to calculate the atomic coordinates for K-dioctahedral micas- $2M_1$ with disordered distribution of tetrahedral and octahedral cations. The estimated standard deviations (e.s.d.) for modeled atomic coordinates vary for different atomic positions and range from 0.0001 to 0.003 (fractional units); the e.s.d. values for structural characteristics obtained from the calculated atomic coordinates are 0.002–0.007 Å for mean and individual tetrahedral bond and edge lengths, 0.004–0.013 Å for mean and individual octahedral bond and edge lengths, 0.013–0.015 Å for K-O distances, and 0.5° for the tetrahedral ditrigonal rotation angle. Computation of atomic coordinates for additional three dioctahedral mica- $2M_1$ structures that were not included in the derivation of the empirical structure-composition relationships used in the algorithm yielded close agreement between the modeled and observed structural characteristics.

The structure modeling algorithm can be used as an inexpensive and express method for evaluation of fine structural features in large collections of K-dioctahedral mica samples of diverse compositions.

Keywords: Crystal structure, modeling, dioctahedral mica, muscovite, phengite, aluminoceladonite

INTRODUCTION

Micas are important and widespread rock-forming minerals that occur in diverse geological environments including sedimentary, metamorphic, and igneous rocks. The mica structure, which has been an object of intense and comprehensive investigation for decades [see, e.g., Brigatti and Guggenheim (2002) and references therein; Ferraris and Ivaldi (2002) and references therein], is described in terms of the mica module, which consists of a 2:1 (or TOT) layer and an interlayer cation. A 2:1 layer consists of two tetrahedral sheets linked through an octahedral sheet, which contains, in the general case, three symmetrically independent sites differing in the arrangement of OH groups and oxygen anions coordinating octahedral cations. In the *trans*-octahedra the OH groups occupy opposite apices, whereas in the *cis*-octahedra the OH groups form a shared edge. The structure of dioctahedral micas is conventionally described in terms of $1M$, $2M_1$, $2M_2$, and $3T$ polytypes differing in mutual arrangement of the adjacent layers (Bailey 1984). The octahedral cations in the 2:1 layers of $2M_1$, $2M_2$, and $3T$ dioctahedral micas typically occupy *cis*-sites only (Bailey 1984; Brigatti and Guggenheim 2002), whereas $1M$ structures may consist of either *trans*-vacant (*tv*) or *cis*-vacant (*cv*) 2:1 layers, or of interstratified layer types (Drits et al. 2006, 2010; Drits and Zviagina 2009). Diverse homovalent and het-

erovalent cation substitutions in both octahedral and tetrahedral sheets of the 2:1 layers of dioctahedral micas lead to substantial variations in their fine structural features.

Despite the considerable progress in the investigation of micas, and potassic dioctahedral micas in particular, certain aspects in their structure, crystal chemistry, and occurrence still remain understudied. No explanation has been found so far for the differences in the composition variations in high- and low-temperature K-dioctahedral micas. In low-temperature K-dioctahedral micas, which normally occur as $1M$ and $1Md$ polytypes, two virtually continuous series can be distinguished, (1) from Mg, Fe-poor illite to aluminoceladonite via Mg-rich illite, and (2) from glauconite to celadonite (Środoń and Eberl 1984; Drits and Kossovskaya 1991; Li et al. 1997; Rieder et al. 1998; Brigatti and Guggenheim 2002; Drits et al. 2006, 2010). In contrast, high-temperature K-dioctahedral $2M_1$ and $3T$ micas form a solid solution between muscovite, $\text{KAl}_2(\text{Si}_3\text{Al})\text{O}_{10}(\text{OH})_2$, and the intermediate member, phengite $\text{KAl}_{1.5}\text{Mg}_{0.5}(\text{Si}_{3.5}\text{Al}_{0.5})\text{O}_{10}(\text{OH})_2$ (Brigatti and Guggenheim 2002; Ferraris and Ivaldi 2002), whereas varieties with cation compositions intermediate between phengite and aluminoceladonite, $\text{KAl}_1\text{Mg}_1\text{Si}_4\text{O}_{10}(\text{OH})_2$, have not been found among natural white dioctahedral micas. It was only possible to synthesize dioctahedral Al, Mg-bearing samples consisting of $2M_1$ and/or $3T$ polytypes with over 3.8 Si per half formula unit (phfu) at extremely high temperature and pressure (over 900°C and about

* E-mail: zbella2001@yahoo.com

10–11 GPa) (Smyth et al. 2000; Schmidt et al. 2001).

A possible way to gain insight into this and similar problems is the application of structure modeling. The structure modeling approach involves derivation of structure/composition relationships that adequately describe the various distortions of the idealized mica structure and are used as a basis for calculating atomic coordinates in dioctahedral micas from the experimental data on cation composition and unit-cell parameters. Numerous authors have studied relationships between structural parameters and cation composition in micas (e.g., Pauling 1930; Radoslovich 1961, 1962; Franzini and Schiaffino 1963; Donnay et al. 1964; Drits 1969, 1975; Tepikin et al. 1969; McCauley and Newham 1971; Hazen and Wones 1972, 1978; Hazen and Burnham 1973; Takeda and Morosin 1975; Appelo 1978; Toraya 1981; Lin and Guggenheim 1983; Bailey 1984; Weiss et al. 1985, 1992; Smoliar-Zviagina 1993; Brigatti and Guggenheim 2002; Brigatti et al. 2003, 2005, 2008; Redhammer and Roth 2002; Mercier et al. 2005, 2006; Drits et al. 2010), and quite a few of these suggested structural models for both dioctahedral and trioctahedral varieties. The majority of the previous models, however, were published before numerous new, high-precision structural data were acquired. A more recent work by Mercier et al. (2005) suggests quite a complicated algorithm for the calculation of atomic coordinates, which has only been validated on $1M$ trioctahedral micas (Mercier et al. 2006). In a study of crystal-chemical variations in low-temperature $1M$ micas in the solid solutions from illite to aluminoceladonite and from glauconite to celadonite, Drits et al. (2010) used a revised version of the algorithm of Smoliar-Zviagina (1993) that was modified to account for new high-precision refined structural data on dioctahedral micas published since 1993. The purpose

of the present paper has been to provide an improved algorithm for the calculation of the unit-cell atomic coordinates in K dioctahedral micas- $2M_1$ from cation composition and unit-cell parameters. Unlike Mercier et al. (2005), the present authors believe that including unit-cell constants as input parameters is essential, as the relations between cell parameters and mica composition are far from being straightforward and need a separate investigation. The new procedure involves changes in the calculation algorithm, as well as further modification of regression equations relating the structural features and chemical composition of micas, which were obtained from the analysis of contemporary published data on refined structures of dioctahedral micas of various compositions. Although the main focus was on K dioctahedral micas- $2M_1$, structures of paragonite- $2M_1$, margarite- $2M_1$, and celadonite- $1M$ were included in the derivation of several regression equations. The data to be included in regression analysis were selected according to the following criteria: high precision in the published structural data ($R < 10\%$); the sum of octahedral cations phfu, Σ_{oct} , from 1.9 to 2.1; overall cation charge phfu, from 21.85 to 22.15; disordered cation distribution. An exception was made for margarite- $2M_1$ (Joswig et al. 1983) having $\Sigma_{\text{oct}} = 2.21$, which was only incorporated in the derivation of the regression for the mean tetrahedral bond length (see below). Micas containing >0.25 atomic units of Li and/or F phfu were excluded as these substitutions affect structural distortions in a complex way that is not altogether clear (Smoliar-Zviagina 1993). Finally, structural data obtained under normal pressure and room temperature were only considered. The cation compositions and the unit-cell parameters of the refined mica structures incorporated in regression analysis are given in Tables 1 and 2.

TABLE 1. Cation compositions (atoms phfu) of the micas incorporated in regression analysis

No.	Sample	Si	^{IV} Al	^{VI} Al	Fe ³⁺	Fe ²⁺	Mg	Ti	Mn ³⁺	Mn ²⁺	Cr	Li	K	Na	Ca	Ba	Total charge	Σ_{oct}	Reference
1	Muscovite- $2M_1$	3.12	0.88	1.88	–	0.14	0.01	–	–	–	–	–	0.85	0.09	–	–	22.0	2.03	Rothbauer (1971)
2	Muscovite- $2M_1$	3.055	0.945	1.718	0.149	–	0.099	0.02	0.02	–	–	–	0.93	0.052	–	–	21.916	2.006	Knurr and Bailey (1986)
3	Muscovite- $2M_1$	3.16	0.84	1.84	0.06	0.01	0.1	–	–	–	–	–	0.79	0.04	0.03	–	21.97	2.01	Tsipursky and Drits (1977)
4	Muscovite- $2M_1$	3.02	0.98	1.9	0.02	0.05	0.06	0.01	–	–	–	–	0.86	0.1	–	–	22.0	2.04	Guggenheim et al. (1987)
5	Muscovite- $2M_1$ (Keystone)	3.1	0.9	1.83	–	0.16	0.01	–	–	–	–	–	0.93	0.06	0.01	–	21.94	2	
6	Muscovite- $2M_1$ (Westland)	3.11	0.89	1.86	–	0.04	0.08	–	–	–	0.06	–	0.86	0.01	0.04	–	22.06	2.04	Brigatti et al. (2001)
7	Muscovite- $2M_1$ (Campbell Creek)	3.07	0.93	1.84	–	0.02	0.02	0.02	–	–	0.1	–	0.72	0.27	–	–	22.04	2	Brigatti et al. (2001)
8	Muscovite- $2M_1$ (B1b)	3.09	0.91	1.83	–	0.07	0.07	0.06	–	–	–	–	0.94	0.06	–	–	22.1	2.03	Brigatti et al. (1998)
9	Muscovite- $2M_1$ (C3-29b)	3.07	0.93	1.88	–	0.07	0.06	0.03	–	–	–	–	0.88	0.06	0.06	–	22.15	2.04	Brigatti et al. (1998)
10	Muscovite- $2M_1$ (GFS-15)	3.03	0.97	1.86	0.01	0.06	0.07	0.02	–	–	–	–	0.92	0.08	–	–	21.98	2.02	Brigatti et al. (1998)
11	Muscovite- $2M_1$ (H87b)	3.09	0.91	1.71	0.16	0.13	–	–	0.01	–	–	–	0.96	0.04	–	–	21.98	2.01	Brigatti et al. (1998)
12	Muscovite- $2M_1$ (A4b)	2.92	1.08	1.88	0.09	–	0.05	0.02	–	–	–	–	0.92	0.08	–	–	22.01	2.04	Brigatti et al. (1998)
13	Muscovite- $2M_1$ (C3-31b)	3.18	0.82	1.64	0.08	0.08	0.16	0.02	–	–	–	–	0.93	0.05	0.01	–	21.9	1.98	Brigatti et al. (1998)
14	Muscovite- $2M_1$ (RA1)	3.18	0.82	1.78	–	0.12	0.06	0.04	–	–	–	–	0.92	0.08	0	–	22.04	2	Brigatti et al. (1998)
15	Fe-rich muscovite- $2M_1$ (GA1)	3.3	0.7	1.65	–	0.29	0	0.01	–	0.07	–	–	0.99	0.01	0	–	22.01	2.02	Brigatti et al. (1998)
16	Fe-rich muscovite- $2M_1$	3.26	0.74	1.67	–	0.34	0.04	0	–	–	–	–	0.94	0.03	0	–	22.0	2.05	Pavese et al. (1999)
17	Mg-rich muscovite- $2M_1$	3.25	0.75	1.51	–	0.15	0.27	0.01	–	–	0.09	–	0.95	0.05	0	–	21.93	2.03	Rule and Bailey (1985)
18	Phengite- $2M_1$ (2M1Y)	3.38	0.62	1.55	–	0.21	0.24	0.02	–	–	–	–	0.98	0.02	0	–	22.01	2.02	Ivaldi et al. (2001)
19	Phengite- $2M_1$ (2M1G)	3.45	0.55	1.42	–	0.24	0.33	0.04	–	–	–	–	0.98	0.02	0	–	22.01	2.03	Ivaldi et al. (2001)
20	Aluminoceladonite- $2M_1$	3.81	0.19	1.21	–	0.04	0.75	–	–	–	–	–	1	–	–	–	22.02	2	Smyth et al. (2000)
21	Paragonite- $2M_1$	2.939	1.051	1.99	–	0.028	0.013	0.003	–	–	–	–	0.042	0.916	–	–	21.931	2.034	Lin and Bailey (1984)
22	Paragonite- $2M_1$	3.01	0.99	1.97	–	0.01	0.006	0.007	–	0.002	–	–	0.1	0.88	0.01	-0.01	22.004	1.995	Comodi and Zanazzi (1997)
23	Paragonite- $2M_1$	2.92	1.08	1.99	–	0.01	0.02	0.005	–	0.001	–	–	0.07	0.91	0.01	0.01	21.992	2.026	Comodi and Zanazzi (2000)
24	Margarite- $2M_1$	2.11	1.89	1.992	–	0.012	0.032	–	–	–	–	–	0.009	0.19	0.812	–	21.997	2.036	Guggenheim and Bailey (1978)
25	Margarite- $2M_1$	1.92	2.08	1.96	0.02	0.01	0.1	0.005	–	–	–	0.115	0	0.21	0.725	–	21.875	2.21	Joswig et al. (1983)
26	Celadonite- $1M$	4	0	0.05	0.96	0.26	0.73	–	–	–	–	–	0.89	–	–	–	21.9	2	Drits et al. (1984)
27	Celadonite- $1M$	3.94	0.06	0.05	1.15	0.36	0.41	0.01	–	–	–	–	0.83	0.01	0.04	–	22.04	1.98	Zhukhlistov (2005)

TABLE 2. Unit-cell parameters of the refined mica structures incorporated in regression analysis (sample numbers as in Table 1)

No.	<i>a</i> (Å)	<i>b</i> (Å)	<i>c</i> (Å)	β (°)	Space group
1	5.1918	9.0155	20.0457	95.735	C2/c
2	5.2044	9.018	20.073	95.82	C2/c
3	5.190	9.000	20.048	95.73	C2/c
4	5.1906	9.008	2.047	95.757	C2/c
5	5.200	9.021	20.07	95.71	C2/c
6	5.192	9.011	20.028	95.74	C2/c
7	5.175	8.979	19.915	95.66	C2/c
8	5.187	9.004	20.036	95.73	C2/c
9	5.188	8.996	20.082	95.78	C2/c
10	5.192	9.013	20.056	95.83	C2/c
11	5.209	9.035	20.066	95.68	C2/c
12	5.186	8.991	20.029	95.77	C2/c
13	5.197	9.022	20.076	95.79	C2/c
14	5.182	8.982	20.002	95.72	C2/c
15	5.226	9.074	20.039	95.74	C2/c
16	5.2140	9.0521	19.9968	95.736	C2/c
17	5.215	9.043	19.974	95.783	C2/c
18	5.225	9.057	19.956	95.73	C2/c
19	5.213	9.051	19.937	95.76	C2/c
20	5.205	9.0368	19.886	95.615	C2/c
21	5.128	8.898	19.287	94.35	C2/c
22	5.135	8.906	19.384	94.6	C2/c
23	5.140	8.911	19.380	94.62	C2/c
24	5.1038	8.8287	19.148	95.46	Cc
25	5.108	8.844	19.156	95.48	Cc
26	5.229	9.051	10.144	100.59	C2
27	5.227	9.053	10.153	100.53	C2/m

STRUCTURAL DISTORTIONS IN THE OCTAHEDRAL AND TETRAHEDRAL SHEETS AND INTERLAYERS OF DIOCTAHEDRAL MICAS

Structural distortions in dioctahedral micas are well-known and have been described in detail by several authors (see Bailey 1984; Brigatti and Guggenheim 2002; and Ferraris and Ivaldi 2002 for reviews). Deviations from the idealized mica structure are determined by various factors, such as tetrahedral/octahedral lateral misfit, compensation of cation-cation repulsion, ordered distribution of vacant octahedral sites, the size and charge of the interlayer cation, and so on. The basic octahedral structural distortions include flattening of the octahedral sheet; counter-rotation of the upper and lower triads of O anions around the *c** axis; differences in the distances from the octahedral cation to hydroxyl and non-hydroxyl oxygen anions; hydroxyl depression, i.e., shift of the adjacent OH groups forming a shared octahedral edge toward each other along *c** by the amount Δ_{OH} to provide shorter M-OH bonds and better screening for the repulsion of the octahedral cations.

To adjust the lateral dimensions of the octahedral and tetrahedral sheets, adjacent tetrahedra are (1) elongated along the *c** axis, so that the mean O–O distance in their basal triads is shorter than that for a tetrahedron of an ideal shape, and (2) rotated in opposite directions around *c** through α leading to ditrigonal symmetry of the tetrahedral sheet. Because of the vacant octahedra being larger than those occupied by cations, the adjacent tetrahedra tilt across the elongated edges of these octahedra, so that the bridging basal oxygen between them moves inside the layer by Δ*Z* with respect to the other two basal oxygen atoms of each tetrahedron

The geometry of the octahedral and tetrahedral coordination sites is often described in terms of various angular parameters, e.g., the octahedral flattening angle, ψ, or tetrahedral elongation angle, τ. For structure modeling purposes, however, these

parameters are inconvenient, as even apparently low errors in the prediction of angular values lead to serious errors in distance parameters and consequently, in atomic coordinates. Preference was given therefore to describing the structural details of the 2:1 layer and interlayer in terms of distance parameters, such as bond and edge lengths and sheet thicknesses, the only exception being the tetrahedral ditrigonal rotation angle, α.

Octahedral sheet

Octahedral bond lengths. Several authors previously suggested equations to predict the mean octahedral bond length in the form $d(\text{M-O,OH}) = \sum c_i d_i$, where *c_i* is the content of each specific cation and *d_i* is the corresponding “partial” metal-oxygen octahedral distance (Drits 1969, 1975; Baur 1981; Weiss et al. 1992; Smoliar-Zviagina 1993; Mercier et al. 2006). Analysis of the high-precision structural data available shows that in dioctahedral micas, the correlation between the mean octahedral bond length *d*(M-O,OH) and the octahedral cation composition can be described by a linear relationship (e.s.d. = 0.003 Å, *r*² = 0.983, p-value <10⁻¹⁰, where e.s.d. is the estimated standard deviation, *r*² is the coefficient of determination, and p-value is the Anova quality of fit):

$$d(\text{M-O,OH}) = (1.918\text{Al} + 2.028\text{Fe}^{3+} + 2.063\text{Fe}^{2+} + 2.065\text{Mg} + 1.900\text{Ti} + 2.000\text{Cr} + 2.000\text{Mn}^{3+} + 2.200\text{Mn}^{2+})/\Sigma_{\text{oct}} \quad (1)$$

where Al, Fe³⁺, etc. are the contents of the corresponding octahedral cations phfu, and Σ_{oct} is the sum of octahedral cations phfu. The coefficients in Equation 1 could be interpreted as “partial” metal-oxygen octahedral distances, but the physical meaning of these values should not be overestimated, because, although they correlate with the respective ionic radii, the correlation is not straightforward. In Figure 1a, the calculated *d*(M-O,OH) values are plotted against the observed mean octahedral bond lengths in refined dioctahedral mica structures. A detailed comparison of the quality of prediction provided by Equation 1 with the equations suggested in previous work (Baur 1981; Weiss et al. 1992; Smoliar-Zviagina 1993; Mercier et al. 2006) is given in Supplemental Discussion.¹

The octahedral cation–non-hydroxyl oxygen distance, *d*(M-O), is, as a rule, longer than the mean octahedral cation–hydroxyl oxygen distance, *d*(M-OH). Based on the concept of Baur (1981) of the dependence of the variations in the individual cation-anion distances on bond-strength sum variations Bookin and Smoliar (1985) showed that the differences between *d*(M-O) and *d*(M-O, OH) can be explained solely by the amount of Al for Si substitution in tetrahedra. The analysis of the contemporary structural data has confirmed the validity of this approach in general but led to re-evaluation of the coefficients in the equation of Smoliar-Zviagina (1993). The modified equation for *d*(M-O) is (e.s.d. = 0.004 Å, *r*² = 0.978, p-value <10⁻¹⁰, Fig. 1b):

$$d(\text{M-O}) = d(\text{M-O,OH}) + 0.0078\text{Si} - 0.0176. \quad (2)$$

¹Deposit item AM-12-095, Supplemental Discussion. Deposit items are available two ways: For a paper copy contact the Business Office of the Mineralogical Society of America (see inside front cover of recent issue) for price information. For an electronic copy visit the MSA web site at <http://www.minisocam.org>, go to the American Mineralogist Contents, find the table of contents for the specific volume/issue wanted, and then click on the deposit link there.

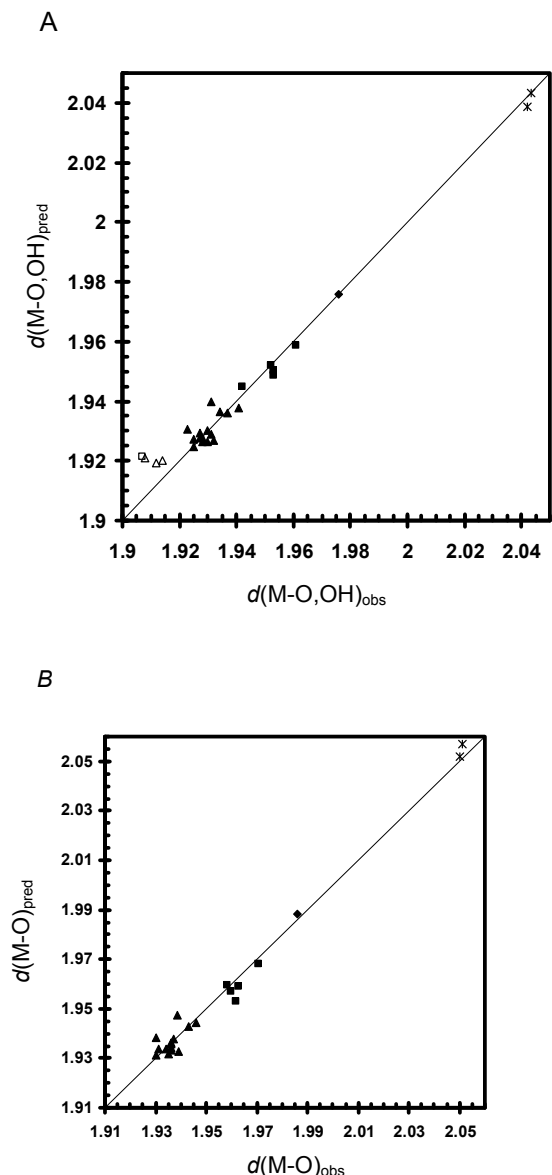


FIGURE 1. Comparison of predicted (a) mean octahedral bond lengths $d(\text{M-O,OH})$ in dioctahedral micas and (b) octahedral cation–non-hydroxyl oxygen distance $d(\text{M-O})$ in K-dioctahedral micas with observed values (Å). Symbols: black triangle = muscovite- $2M_1$, black square = Fe- and/or Mg-rich muscovite and phengite- $2M_1$, diamond = aluminoceladonite- $2M_1$, open triangle = paragonite- $2M_1$, open square = margarite- $2M_1$, asterisk = celadonite- $1M$.

Hereinafter $d(\text{M-O,OH})$ is given by Equation 1 and Si is the amount of Si cations pfu. Analysis of contemporary structural data confirms the observation of Smoliar-Zviagina (1993) that one of the two symmetrically independent octahedral cation–non-hydroxyl oxygen distances is normally longer than the other and the ratio between them is close to 1:0.99. The longer M-O distance is therefore given by

$$d(\text{M-O})_{\text{long}} = 2d(\text{M-O})/1.99. \quad (3)$$

Octahedral sheet thickness. Because the adjacent OH groups forming a shared octahedral edge are shifted toward each other along c^* by the amount Δ_{OH} to provide shorter M-OH bonds and better screening for the repulsion of octahedral cations (Drits et al. 2006), the octahedral sheet is characterized by two thickness values, $\langle h_{\text{oct}} \rangle$ and $h_{\text{oct}}^{\text{max}}$. Here $\langle h_{\text{oct}} \rangle$ is the thickness of the octahedral sheet averaged over all the anions, and $h_{\text{oct}}^{\text{max}} = \langle h_{\text{oct}} \rangle + 2\Delta_{\text{OH}}/3$ is the distance along c^* between the upper and lower apical (i.e., non-hydroxyl) oxygen atoms in an octahedron. The mean octahedral thickness is given by the equation (e.s.d. = 0.007 Å, $r^2 = 0.998$, p-value $< 10^{-10}$, Fig. 2)

$$\langle h_{\text{oct}} \rangle = 1.4743 d(\text{M-O,OH}) - 0.0835b \quad (4)$$

where b is the unit-cell parameter. The OH-depression can be predicted as

$$\Delta_{\text{OH}} = 0.071 - 0.050 \text{Fe}^{2+} - 0.076 \text{Mg} \quad (5)$$

(e.s.d. = 0.005 Å, $r^2 = 0.928$, p-value $< 10^{-10}$, Fig. 3).

Position of the octahedral cation. With increasing contents of divalent octahedral cations the hexagonal pattern in the arrangement of the octahedral cations in $2M_1$ micas becomes slightly distorted because the cations tend to move closer to the shared OH-OH edges. A possible reason for this distortion may be the need to ensure better compensation of the undersaturated charge on hydroxyl O atoms resulting from the formation of hydrogen bonds between the hydroxyl H and the nearest O anions. As a result, the fractional x and y coordinates of the octahedral cation deviate from the idealized values of 1/4 and 1/12, so that

$$x_M = 1/4 + 0.00031\text{Al} + 0.00129\text{Fe}^{3+} - 0.00600\text{Fe}^{2+} - 0.00562\text{Mg} \quad (6a)$$

(e.s.d. = 0.0006, $r^2 = 0.762$, p-value $< 10^{-7}$, Fig. 4a);

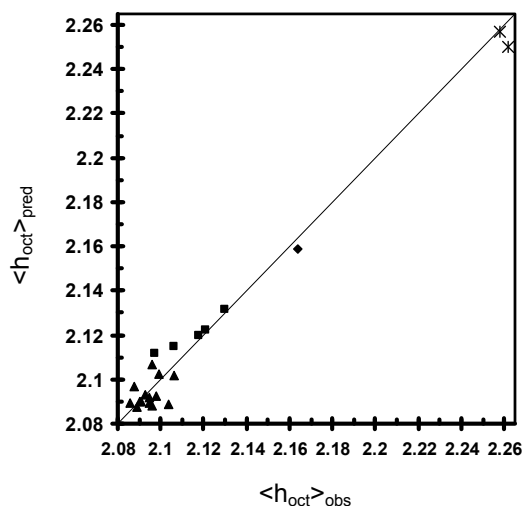


FIGURE 2. Comparison of predicted and observed mean octahedral sheet thickness values, $\langle h_{\text{oct}} \rangle$, (Å) in K-dioctahedral micas. Symbols: black triangle = muscovite- $2M_1$, black square = Fe- and/or Mg-rich muscovite and phengite- $2M_1$, diamond = aluminoceladonite- $2M_1$, asterisk = celadonite- $1M$.

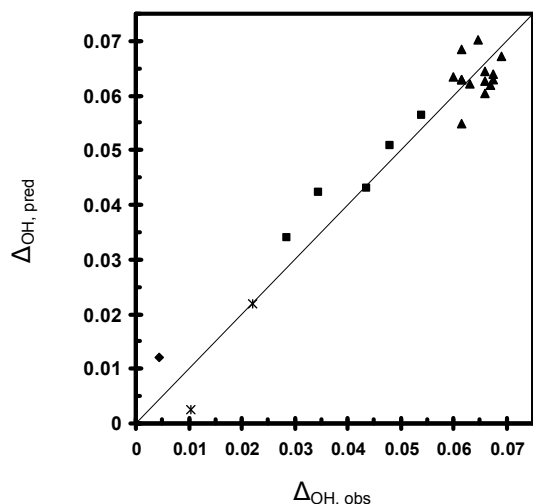


FIGURE 3. Comparison of predicted and observed OH-depression values Δ_{OH} (Å) in K-dioctahedral micas (symbols as in Fig. 2).

$$y_M = 1/12 + 0.00013Al - 0.00145Fe^{2+} - 0.00252Mg \quad (6b)$$

(e.s.d. = 0.0002, $r^2 = 0.857$, p-value $< 10^{-10}$, Fig. 4b).

Tetrahedral sheet

Tetrahedral bond lengths. Several linear equations have been previously suggested to relate the mean T-O distance, d_T , and Al (and/or Fe) for Si substitution in micas (e.g., Hazen, and Burnham 1973; Drits 1969, 1975; Baur 1981; Brigatti and Guggenheim 2002). For dioctahedral micas, however, these relationships tend to underestimate the d_T values when the tetrahedral Al content is low (0 to 0.2 apfu), as in celadonite and aluminoceladonite). The variations in d_T for dioctahedral micas ranging in composition from celadonite to margarite (with tetrahedral Al content of about 2 apfu) is best described by a non-linear dependence (e.s.d. = 0.003 Å, $r^2 = 0.958$, p-value $< 10^{-10}$, Fig. 5a):

$$d_T = 1.6192 + 0.1569 (^{IV}Al/4)^{1.25} \quad (7)$$

where ^{IV}Al is the amount of Al cations in tetrahedra (phfu). (No examples of Fe for Si substitutions in refined dioctahedral mica structures have been reported so far.) The different previous equations for predicting d_T are compared with Equation 7 in Supplemental Discussion¹.

Individual T-O distances can significantly deviate from the mean values. These deviations are sometimes described in terms of the displacement of the tetrahedral cation from the geometrical center of the tetrahedron (Brigatti and Guggenheim 2002; Mercier et al. 2005). For structure modeling purposes, however, we find it more convenient to consider the differences between the non-bridging ($T-O_{apical}$) and mean bridging ($T-O_{basal}$) tetrahedral cation-anion distances ($d_{nbr}-d_{br}$), all the more that the actual tetrahedral shape is normally far from regular. Bookin and Smoliar (1985) and Smoliar-Zviagina (1993) suggested an empirical equation relating ($d_{nbr}-d_{br}$) with the bond strength sum variation $\Delta p_i = p_i - \langle p \rangle$, where p_i is the sum of bond strengths received by the anion i and $\langle p \rangle$ is the average bond strength sum

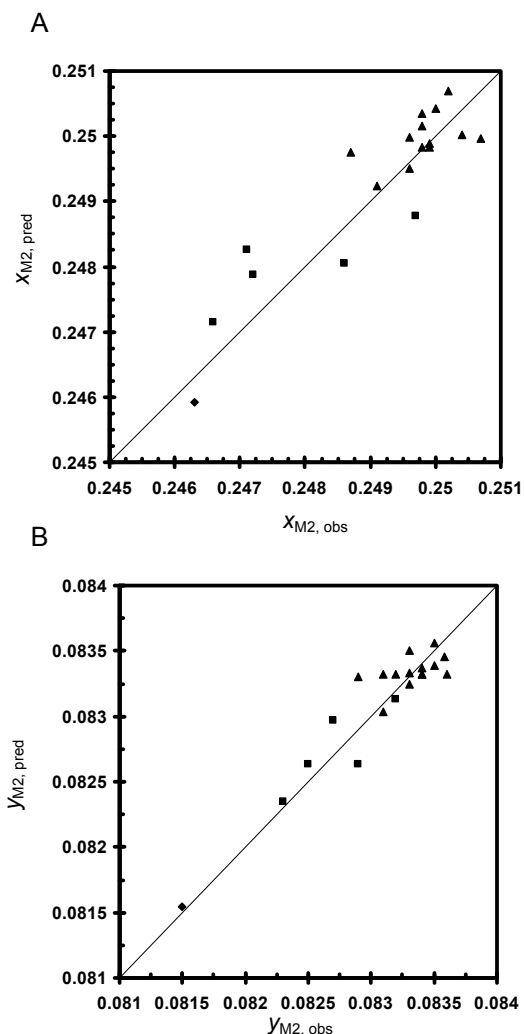


FIGURE 4. Comparison of predicted and observed (a) x and (b) y fractional coordinates of the octahedral cation in K-dioctahedral micas-2M₁. Symbols: black triangle = muscovite-2M₁, black square = Fe- and/or Mg-rich muscovite and phengite-2M₁, diamond = aluminoceladonite-2M₁.

for the coordination polyhedron (Baur 1981). When applied to contemporary structural data this equation describes reasonably well the tetrahedral cation-anion distances in phengites and aluminoceladonite but systematically underestimate the $d_{nbr}-d_{br}$ values in muscovites. A possible way to overcome this inconsistency could be to use the equation of Smoliar-Zviagina (1993) for phengites and aluminoceladonite, whereas for muscovites, to assume $d_{nbr} = d_T$, as the standard deviation of the observed d_{nbr} values from d_T for muscovites is 0.003 Å. This approach, however, has been discarded, as the boundary between muscovite and phengite is rather ambiguous. An alternative strategy has been to find a unique dependence that would describe adequately the bond length variations for the whole range of tetrahedral cation compositions. This dependence was sought in the form $d_{nbr} - d_T = a_1 + (^{IV}Al/4)(a_2\Delta p + a_3\Delta p^2)$, which, in fact is the generalized equation of Smoliar-Zviagina (1993) and reflects assumptions that (1) the individual bond length variations differ in Si- and

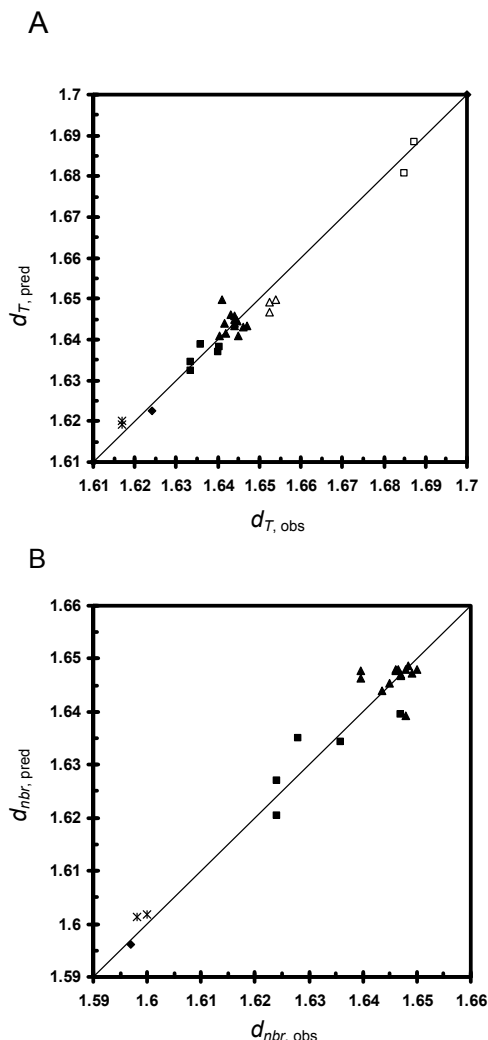


FIGURE 5. Comparison of observed and predicted (a) mean tetrahedral bond lengths d_T (Å) in muscovites, phengites, aluminoceladonite, paragonites, margarites $2M_1$, and celadonites $1M$ and (b) non-bridging bond lengths d_{nbr} (Å) in K-dioctahedral micas (symbols as in Fig. 1).

Al-tetrahedra and (2) there is an effective additional positive bond valence contribution on the apical oxygen anion, which is needed to account for d_{nbr} being greater than or equal to d_T in quite a few structures.

The bond strength sum variation is given by $\Delta p = p_{01,2} - \langle p \rangle = Q_{oct}/4 - 3Q_T/16 - Q_{IC}/8$, where $p_{01,2}$ is the bond strength sum for the apical oxygen anion, $\langle p \rangle$ is the average bond strength sum for the tetrahedron, Q_{oct} , Q_T , and Q_{IC} are the mean octahedral, tetrahedral, and interlayer charges, respectively.

Regression analysis provided the following equation

$$d_{nbr} - d_T = -0.017 - (Al^{IV}/4)(2.264\Delta p + 13.179\Delta p^2) \quad (8)$$

which, despite the complicated form, provides high predictive accuracy (e.s.d. = 0.003 Å, $r^2 = 0.896$, p-value $< 10^{-8}$, Fig. 5b).

Tetrahedral edge lengths. Tetrahedral elongation and, accordingly, the shortening of the basal tetrahedral edge lengths are related to mica cation composition. The relationship between

the mean basal tetrahedral edge length and tetrahedral Al and Fe suggested by Brigatti and Guggenheim (2002) predicts the basal tetrahedral edge lengths in dioctahedral $2M_1$ micas with e.s.d. = 0.008 Å. More accurate prediction is provided by the modified equation of Smoliar-Zviagina (1993), which takes into account both the tetrahedral and interlayer cation composition (e.s.d. = 0.004 Å, $r^2 = 0.920$, p-value $< 10^{-10}$, Fig. 6a):

$$l_b = d_T(1.633 - 0.003Si - 0.010K) \quad (9)$$

where l_b is the mean basal tetrahedral edge length, d_T is given by Equation 7, and Si and K are the amounts of respective cations pfhu. The apical edge length is then given by $l_{ap} = 2\sqrt{3}d_T - l_b$.

In dioctahedral micas- $2M_1$, two of the six symmetrically independent basal edges, namely, those forming the smaller angle in the ditrigonal ring with the vertex at the depressed oxygen anion, are elongated. Similar elongation of two basal tetrahedral edge lengths is observed in celadonite- $1M$ (Zhukhlistov 2005), but not in the celadonite- $1M$ sample studied by Drits et al. (1984). This elongation cannot be assumed constant, as supposed previously (Smoliar-Zviagina 1993),

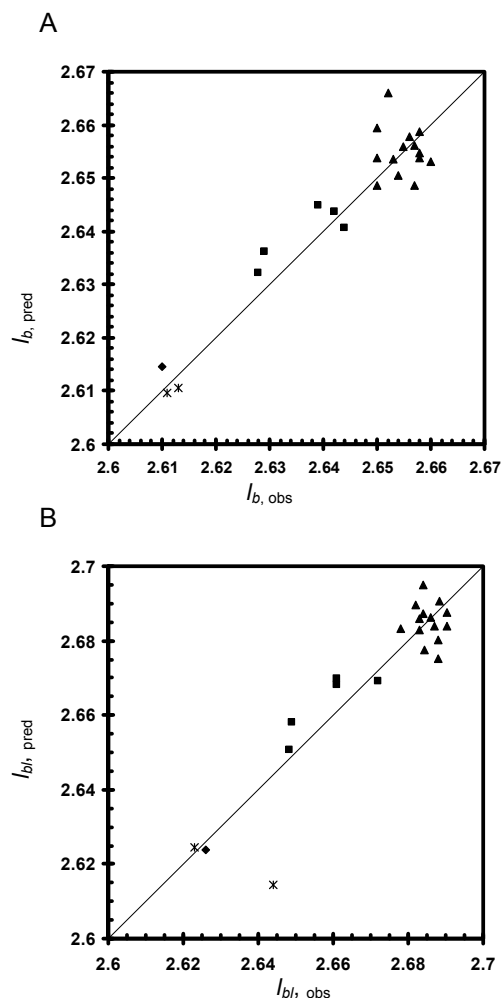


FIGURE 6. Comparison of predicted and observed (a) mean tetrahedral basal and (b) elongated tetrahedral basal edge lengths (l_b and l_{bt} , Å) in K-dioctahedral micas (symbols as in Fig. 2).

but depends on the octahedral cation composition, so that

$$l_{bl} - l_b = 0.033 - 0.03Mg - 0.019Fe^{2+} \quad (10)$$

(e.s.d. = 0.007 Å, $r^2 = 0.459$, p-value = 0.002, Fig. 6b), where l_b is given by Equation 9. Although in Equation 10, $r^2 < 0.80$, the correlation coefficient between the calculated and observed values of l_{bl} is $r^2 = 0.897$.

Tetrahedral basal surface corrugation and sheet thickness. Smoliar-Zviagina (1993) and Brigatti and Guggenheim (2002) obtained regression equations relating ΔZ with the differences between the sizes of vacant and occupied cations. Using such relationships in a structure model is, however, problematic because of the uncertainty in predicting the size of the vacant octahedron. Drits et al. (2010) suggested a relationship between ΔZ and the contents of octahedral Al and Fe^{3+} cations, which allows predicting ΔZ values with e.s.d. = 0.008 Å. The dependence of ΔZ on the octahedral cation composition and the difference between the sizes of vacant and occupied octahedra is implicitly expressed in a relationship between ΔZ , the octahedral cation – non-hydroxyl oxygen distance $d(M-O)$, and b :

$$\Delta Z = 4.0553 - 1.4956 d(M-O) - 0.1050 b. \quad (11)$$

With $d(M-O)$ given by Equation 2, Equation 11 describes the observed ΔZ values with e.s.d. = 0.005 Å, $r^2 = 0.991$, and p-value $< 10^{-10}$ (Fig. 7).

The tetrahedral sheet thickness can be characterized by two values, h_T^{\max} and h_T^{\min} , as calculated over the non-depressed and depressed oxygen anions, respectively ($h_T^{\max} = h_T^{\min} + \Delta Z$). Analysis of the published structural data shows that there is a strong linear correlation between h_T^{\max} and ΔZ .

$$h_T^{\max} = 2.2017 + 0.4392 \Delta Z \quad (12a)$$

(e.s.d. = 0.006 Å, $r^2 = 0.917$, p-value $< 10^{-10}$)

(with observed values of ΔZ) and

$$h_T^{\max} = 2.2315 + 0.2945 \Delta Z$$

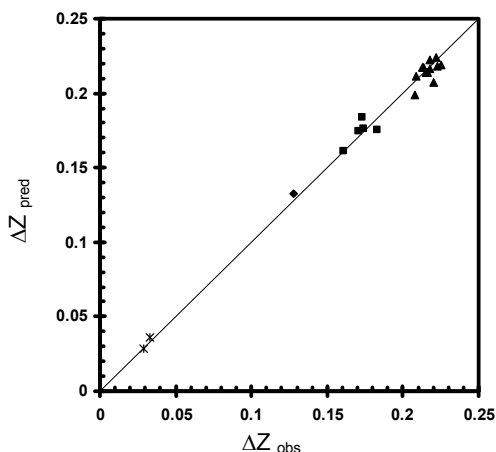


FIGURE 7. Comparison of predicted and observed values for tetrahedral basal surface corrugation ΔZ (Å) in K-dioctahedral micas (symbols as in Fig. 2).

$$(e.s.d. = 0.005 \text{ \AA}, r^2 = 0.738, p\text{-value} < 10^{-5}, \text{ Fig. 8}) \quad (12b)$$

(with ΔZ given by Eq. 11). The mean tetrahedral sheet thickness is given by $\langle h_T \rangle = (2h_T^{\max} + h_T^{\min})/3$.

Tetrahedral rotation. The rotation of adjacent tetrahedra around the c^* axis by the α angle that allows the lateral adjustment of the octahedral and tetrahedral sheets depends on many structural parameters of both sheets (Bailey 1984; Weiss et al. 1992; Smoliar-Zviagina 1993; Brigatti and Guggenheim 2002; Drits et al. 2010). In general, substitution of smaller trivalent for larger divalent octahedral cations and the simultaneous decrease in the tetrahedral Al content improves the fit between the sheets and consequently decreases the tetrahedral rotation angle α . Brigatti and Guggenheim (2002) suggested that tetrahedral rotation in micas was related to the ratio of basal tetrahedral and lateral octahedral edge lengths so that $\cos \alpha = (\sqrt{3}/2)k$, where k is the ratio of the mean octahedral lateral O-O distance (taking into account the vacant octahedron) to the mean basal tetrahedral edge length. Figures 13 and 14 in Brigatti and Guggenheim (2002) show that for the range of α values from about 5° to about 10° , the scatter of the points is up to 3° when the observed edge lengths are used, and up to $6-8^\circ$ using the empirical relationships suggested by the authors. Analysis of the published refined structural data shows that a more accurate prediction of α in K-dioctahedral micas $2M_1$ is given by

$$\alpha = \arcsin(0.8672b/3l_b) \quad (13)$$

(e.s.d. = 0.5° , $r^2 = 0.952$, p-value $< 10^{-10}$, Fig. 9),

where l_b is given by Equation 9. The accuracy provided by Equation 13 is comparable to albeit slightly higher than that of a linear dependence between α and $Al^{IV} + Al^{VI}$ obtained by Brigatti et al. (2005), when applied to the set of samples used in the present study (e.s.d. = 0.6° , $r^2 = 0.931$).

Position of the interlayer cation

The position of the interlayer cation is determined by the coordinate Y_A , as $X_A = 0$, and $Z_A = c \sin \beta / 4$. The interlayer cation is shifted along b from the idealized position of $1/12$ toward the

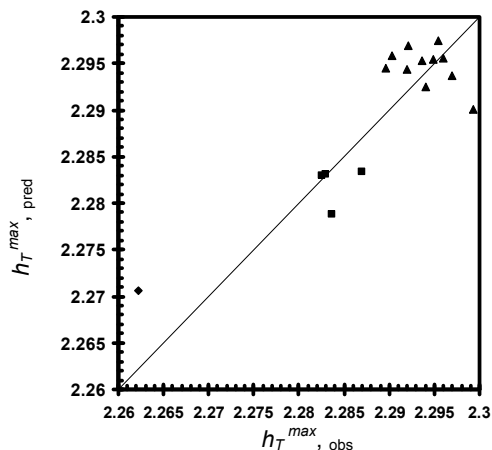


FIGURE 8. Comparison of predicted and observed values for maximum tetrahedral sheet thickness h_T^{\max} (Å) in K-dioctahedral micas- $2M_1$ (symbols as in Fig. 4).

depressed tetrahedral basal oxygen anion, O4, so that there is a nearly linear dependence between the distance A-O4 (inner) and the mean inner $\langle A-O \rangle_{in}$ distance (Fig. 10):

$$A-O4 = 1.007 \langle A-O \rangle_{in} \quad (\text{e.s.d.} = 0.004 \text{ \AA}, r^2 = 0.94, \text{ p-value} < 10^{-10}). \quad (14)$$

Statistical significance of the regression equations

For all the above regressions, the p-values are well below the common significance threshold of 0.05; in most cases, the r^2 parameter exceeds 80%. Equations 6a, 10, and 12b are exceptions, with $r^2 < 0.8$. The relatively low $r^2 = 0.762$ in the dependence of x_M on the octahedral cation composition may be explained by the fact that the majority of structures included in the analysis are muscovites, where the x_M values are, at the same time, very close to and randomly scattered around 0.25 (Fig. 4a). The very low (< 0.5) r^2 in Equation 10 relating the elongation of one of the basal tetrahedral edges ($l_{bl} - l_b$) with the contents of divalent octahedral cations may be associated with the low values of

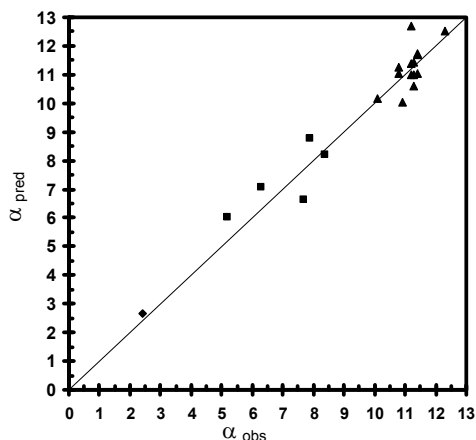


FIGURE 9. Comparison of predicted and observed values for tetrahedral ditrigonal rotation angle α ($^\circ$) in K-dioctahedral micas- $2M_1$ (symbols as in Fig. 4).

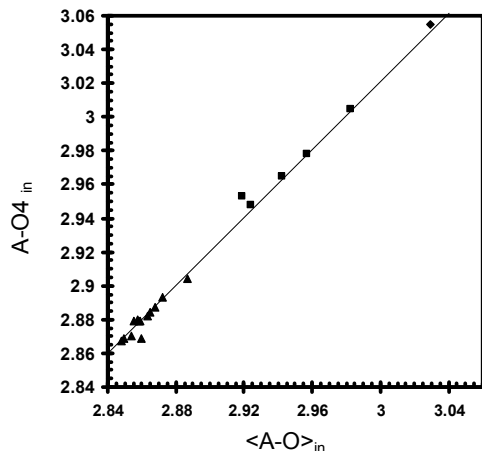


FIGURE 10. The A-O4 distance (inner) plotted against the mean inner $\langle A-O \rangle_{in}$ distance (\AA) for refined structures of K-dioctahedral micas- $2M_1$ (symbols as in Fig. 4).

Mg and Fe^{2+} in most samples. At the same time, the correlation coefficient between the calculated and observed values of l_{bl} is $r^2 = 0.897$. The parameter $r^2 = 0.917$ for Equation 13a shows that there is a strong correlation between the observed values of h_T^{max} and ΔZ . Replacing the observed ΔZ by the value obtained from Equation 11, however, reduces r^2 to 0.738 for Equation 12b. Nevertheless, the three regressions in question provide acceptable standard errors: ± 0.0006 fractional units (equivalent to $\sim 0.003 \text{ \AA}$), ± 0.007 and $\pm 0.005 \text{ \AA}$, respectively.

CALCULATION OF THE ATOMIC COORDINATES

The input parameters for the calculation of the Cartesian atomic coordinates are the unit-cell parameters a , b , c (\AA), and β ($^\circ$) and the contents of the tetrahedral, octahedral, and interlayer cations (phfu). At the first stage, Equations 1–11, 12b, 13, and 14 are used to calculate $d(\text{M-O,OH})$, $d(\text{M-O})$, $d(\text{M-O})_{\text{long}}$, $\langle h_{\text{oct}} \rangle$, Δ_{OH} , $h_{\text{oct}}^{\text{max}}$, x_M , y_M , d_T , d_{hts} , d_{hts} , l_b , l_{bl} , ΔZ , h_T^{max} , h_T^{min} , α^{pred} (given by Eq. 13, as distinct from α^{calc} calculated from the atomic coordinates in the structure model), and A-O4. At the second stage, the atomic coordinates for all the symmetrically independent atomic sites in the unit-cell of a dioctahedral mica $2M_1$ (Fig. 11) are computed using formulas obtained from relevant geometric constructions (Table 3; Fig. 12–15). In Table 3, the coordinates of the atomic sites are given in the order they are calculated in the algorithm. The derivations of the formulas are illustrated in Figures 12 to 15; the additional parameters are explained below.

Oxygen anions common to octahedral and tetrahedral sheets, O1 and O2, and the hydroxyl oxygen site, OH

The parameters $r(\text{M-O})_{\text{short}}$, $r(\text{M-O})_{\text{long}}$, and $r(\text{M-OH})$ are projections of the longer and shorter M-O distances, and the M-OH distance, respectively, on the ab plane (Fig. 12)

$$r(\text{M-O})_{\text{long}} = \sqrt{d(\text{M-O})_{\text{long}}^2 - \frac{(h_{\text{oct}}^{\text{max}})^2}{4}}$$

$$r(\text{M-O})_{\text{short}} = \sqrt{d(\text{M-O})_{\text{short}}^2 - \frac{(h_{\text{oct}}^{\text{max}})^2}{4}},$$

where $d(\text{M-O})_{\text{short}} = 0.99d(\text{M-O})_{\text{long}}$ is the shorter M-O distance;

$$r(\text{M-OH}) = \sqrt{d(\text{M-OH})^2 - \frac{(h_{\text{oct}}^{\text{min}})^2}{4}}.$$

The angles σ_1 , σ_2 , $\Delta\sigma$, and σ_{OH} are obtained from the relevant triangles in Figure 12 as

$$\sigma_1 = \arccos \left[\frac{r(\text{M-O})_{\text{long}}^2 - r(\text{M-O})_{\text{short}}^2 - (a - 2X_M)^2 - 4Y_M^2}{2r(\text{M-O})_{\text{short}} \sqrt{(a - 2X_M)^2 + 4Y_M^2}} \right];$$

$$\sigma_2 = \arccos \left[\frac{r(\text{M-O})_{\text{short}}^2 - r(\text{M-O})_{\text{long}}^2 - \left(\frac{b/2 - 2Y_M}{\cos \Delta\sigma} \right)^2}{2r(\text{M-O})_{\text{long}} \frac{b/2 - 2Y_M}{\cos \Delta\sigma}} \right];$$

$$\Delta\sigma = \arctan \frac{a/2 - 2X_M}{b/2 - 2Y_M};$$

$$\sigma_{\text{OH}} = \arccos \frac{\sqrt{X_M^2 + Y_M^2}}{r(\text{M-OH})}$$

Here and in Table 3, X_i , Y_i , and Z_i ($i = \text{K}, \text{M}, \text{O1}, \text{O2}, \text{O3}, \text{O4}, \text{T1}, \text{T2}$) are the Cartesian coordinates of the corresponding atoms in absolute units. The value $h_{\text{OCT}}^{\text{min}}$ used to calculate Z_{OH} is the octahedral sheet thickness calculated over the hydroxyl oxygen anions given by $h_{\text{OCT}}^{\text{min}} = h_{\text{OCT}}^{\text{max}} - 2\Delta_{\text{OH}}$.

Basal oxygen anions

The parameter $d(\text{O1-O2})$ used in the calculation of the calculation of the X and Y coordinates of the depressed basal oxygen, O4, is the distance between atoms O1 and O2 (Fig. 13):

$$d(\text{O1-O2}) = \sqrt{(X_{\text{O1}} + a/2 - X_{\text{O2}})^2 + (Y_{\text{O1}} + b/2 - Y_{\text{O2}})^2};$$

The angle δ_1 , as follows from Figure 13, is given by

$$\delta_1 = \arctan \left(\frac{Y_{\text{O1}} + b/2 - Y_{\text{O2}}}{X_{\text{O1}} + a/2 - X_{\text{O2}}} \right) - \alpha^{\text{pred}}.$$

The X and Y coordinates of the non-depressed basal O atoms, O3, and O5, are derived from the relevant triangles in Figure 13.

Tetrahedral cations, T1 and T2

The parameters r'_{br} and r''_{br} are projections, on the a - b plane, of the distances between the tetrahedral cation and the depressed and non-depressed basal oxygen anion, respectively (Fig. 14):

$$r''_{br} = \sqrt{d_{br}^2 - (Z_{\text{O4}} - Z_T)^2};$$

$$r'_{br} = \sqrt{d_{br}^2 - (Z_{\text{O5}} - Z_T)^2}$$

The angles δ_2 and δ_3 are derived from the relevant triangles in Figure 14

$$\delta_2 = \arccos \left(-\frac{(r'_{br})^2 - (r''_{br})^2 - r(\text{O4-O5})^2}{2r''_{br}r(\text{O4-O5})} \right)$$

$$\delta_3 = \arccos \left(-\frac{(r'_{br})^2 - (r''_{br})^2 - r(\text{O3-O4})^2}{2r''_{br}r(\text{O3-O4})} \right)$$

where $r(\text{O4-O5}) = \sqrt{(X_{\text{O5}} + a - X_{\text{O4}})^2 + (Y_{\text{O5}} - Y_{\text{O4}})^2}$ and

$r(\text{O3-O4}) = \sqrt{(X_{\text{O4}} - X_{\text{O3}})^2 + (Y_{\text{O4}} - Y_{\text{O3}})^2}$ are projections of the O4-O5 and O3-O4 distances on the ab plane.

The Z coordinate of the tetrahedral cation ($Z_{\text{T1}} = Z_{\text{T2}} = Z_T$) is derived from the section of the T1 tetrahedron by a plane passing through the edge O1-O4 normal to the ab plane (Fig. 15). The angles θ_1 and θ_2 are given by

TABLE 3. Formulas for calculating Cartesian atomic coordinates for K-dioctahedral mica 2M₁ unit cell, space group C2/c (see text for explanations)

Atomic position	X	Y	Z
M	$x_M a$	$y_M b$	0
O1	$X_M + r(\text{M-O})_{\text{short}} \cos(\sigma_1 + \arctan \frac{2Y_M}{a - 2X_M})$	$Y_M - r(\text{M-O})_{\text{short}} \sin(\sigma_1 + \arctan \frac{2Y_M}{a - 2X_M})$	$\frac{h_{\text{OCT}}^{\text{max}}}{2}$
O2	$X_M + r(\text{M-O})_{\text{long}} \sin(\sigma_2 + \Delta\sigma)$	$Y_M + r(\text{M-O})_{\text{long}} \cos(\sigma_2 + \Delta\sigma)$	$\frac{h_{\text{OCT}}^{\text{max}}}{2}$
OH	$X_M - r(\text{M-OH}) \sin(\sigma_{\text{OH}} + \arctan \frac{X_M}{Y_M})$	$Y_M - r(\text{M-OH}) \cos(\sigma_{\text{OH}} + \arctan \frac{X_M}{Y_M})$	$\frac{h_{\text{OCT}}^{\text{min}}}{2}$
O4	$X_{\text{O2}} + (\frac{d(\text{O1-O2})}{2 \cos \alpha^{\text{pred}}}) \cos \delta_1 + 0.0029a$	$Y_{\text{O2}} + (\frac{d(\text{O1-O2})}{2 \cos \alpha^{\text{pred}}}) \sin \delta_1 - 0.0026b$	$Z_{\text{O1}} + h_T^{\text{min}}$
O3	$X_{\text{O4}} + \sqrt{l_{bl}^2 - (\Delta Z)^2} \sin(30^\circ - \alpha^{\text{pred}}) - a/2 + 0.0011a$	$Y_{\text{O4}} + \sqrt{l_{bl}^2 - (\Delta Z)^2} \cos(30^\circ - \alpha^{\text{pred}}) - b/2 - 0.0022b$	$Z_{\text{O4}} + \Delta Z$
O5	$X_{\text{O4}} - \sqrt{l_{bl}^2 - (\Delta Z)^2} \cos \alpha^{\text{pred}} + 0.0036a$	$Y_{\text{O4}} - \sqrt{l_{bl}^2 - (\Delta Z)^2} \sin \alpha^{\text{pred}} - 0.0021b$	$Z_{\text{O4}} + \Delta Z$
T1	$X_{\text{O4}} + r'_{br} \cos(\delta_2 + \alpha^{\text{pred}}) + 0.0015a$	$Y_{\text{O4}} + r'_{br} \sin(\delta_2 + \alpha^{\text{pred}}) - 0.0024b$	$Z_{\text{O1}, \text{O2}} + d_{nbr} \sin(\theta_1 + \theta_2)$
T2	$X_{\text{O4}} - r''_{br} \sin(\delta_3 + 30^\circ + \alpha^{\text{pred}}) + 0.0032a$	$Y_{\text{O4}} - r''_{br} \cos(\delta_3 + 30^\circ + \alpha^{\text{pred}}) - 0.0016b$	$Z_{\text{O1}, \text{O2}} + d_{nbr} \sin(\theta_1 + \theta_2)$
A	0	(see text)	$c \sin \beta / 4$

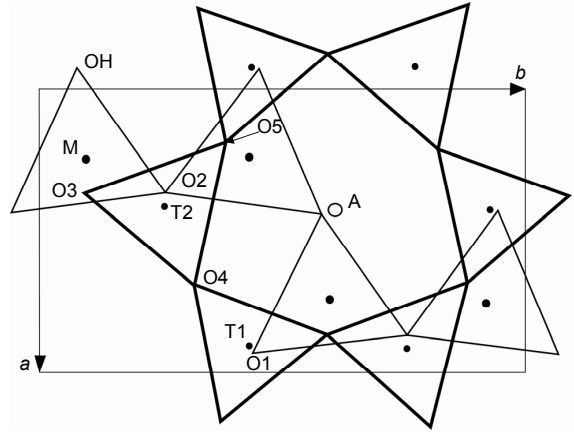


FIGURE 11. Fragment of the unit cell of a dioctahedral mica-2M₁ projected on the ab plane. A = interlayer cation site; M = octahedral cation site; T1, T2 = tetrahedral cation sites; O1, O2 = apical oxygen sites; O3, O4, O5 = basal oxygen sites; OH = hydroxyl oxygen site.

$$\theta_1 = \arcsin \left(\frac{h_T^{\text{min}}}{d(\text{O1-O4})} \right)$$

$$\theta_2 = \arccos \left(-\frac{d_{br}^2 - d_{nbr}^2 - d(\text{O1-O4})^2}{2d_{nbr}d(\text{O1-O4})} \right)$$

where

$$d(\text{O1-O4}) = \sqrt{\left(\frac{d(\text{O1-O2})}{2 \cos \alpha^{\text{pred}}} \right)^2 + (h_T^{\text{min}})^2}$$

is the O1-O4 edge length. Additional terms (0.0015a, 0.0024b etc.) are included in the formula for the X and Y coordinates of atoms T1, T2, O3, O4, and O5 (Table 2) because, as shown by the comparison of the calculated atomic coordinates with the corresponding observed values in 20 refined K-dioctahedral micas-2M₁, the x coordinates of these sites are systematically underestimated, on average, by 0.0015, 0.0032, 0.0011, 0.0029,

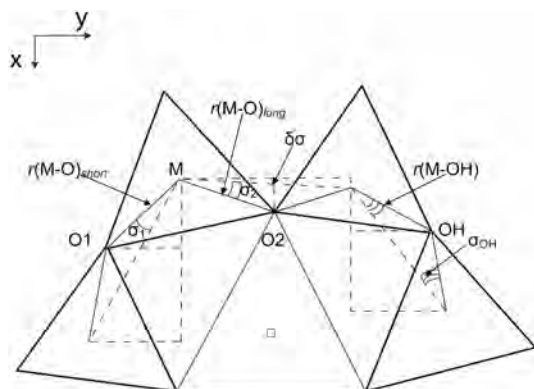


FIGURE 12. Fragment of the octahedral sheet of a dioctahedral mica- $2M_1$ projected on the ab plane: Calculation of X and Y coordinates for M , $O1$, $O2$, and OH .

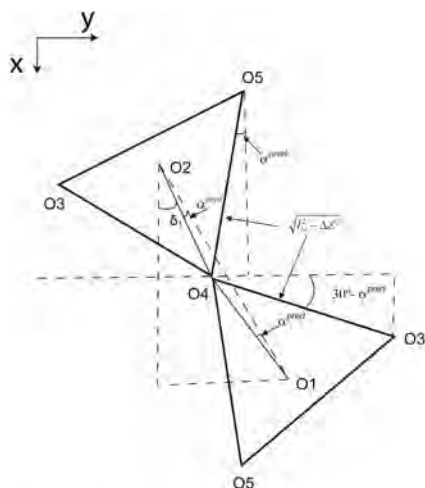


FIGURE 13. Adjacent $T1$ and $T2$ tetrahedra projected on the ab plane: Calculation of X and Y coordinates for $O4$, $O3$, and $O5$.

and 0.0036 (fractional units), respectively, and their y coordinates are systematically overestimated, on average, by 0.0024, 0.0016, 0.0022, 0.0026, and 0.0021 (fractional units), respectively.

Interlayer cation

The Y_A coordinate is first assigned arbitrarily to estimate the mean inner A-O distance, $\langle A-O \rangle_{in}$. Then, Y_A is adjusted to satisfy Equation 14.

RESULTS AND DISCUSSION

The above algorithm was used to obtain structure models for 20 K-dioctahedral micas- $2M_1$ (space group $C2/c$). The refined and modeled fractional monoclinic atomic coordinates for all the selected mica samples are compared in Appendix Table 1 (sample numbers are the same as in Table 1). The e.s.d. values for modeled x , y , and z given in parentheses vary for different atomic positions and range from 0.0001 to 0.003 (fractional units); the e.s.d. values for the experimental values are given in the respective publications. To facilitate comparison, the experimental coordinates have been rounded to four digits.

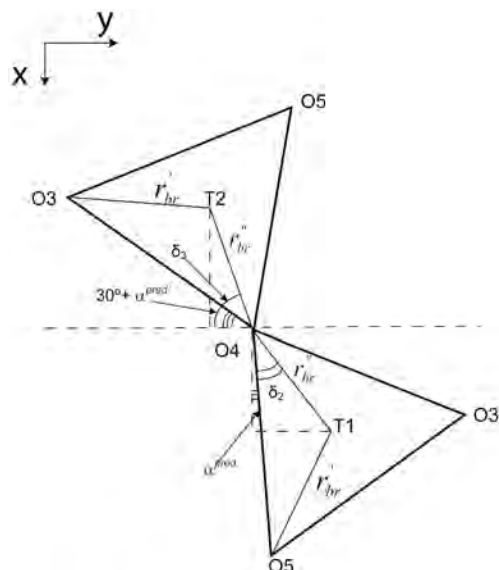


FIGURE 14. Adjacent $T1$ and $T2$ tetrahedra projected on the ab plane: Calculation of X and Y coordinates for $T1$ and $T2$.

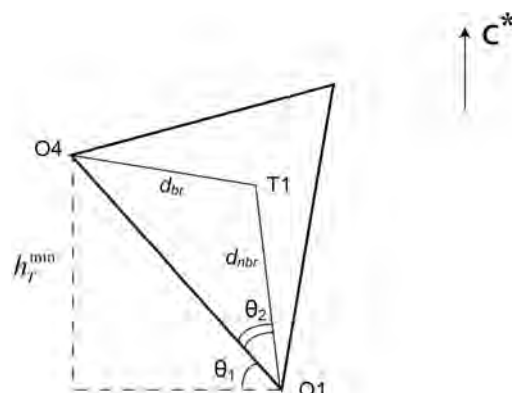


FIGURE 15. Section of the $T1$ tetrahedron by a plane passing through the edge $O1-O4$ normal to the ab plane: Calculation of the Z coordinate of the tetrahedral cation.

Comparison of the 20 structure models with the corresponding refined structural data provided the following e.s.d. values for the structure details obtained from the calculated atomic coordinates: 0.002–0.007 Å for mean and individual tetrahedral bond and edge lengths, 0.004–0.013 Å for mean and individual octahedral bond and edge lengths, 0.013–0.015 Å for A-O distances, and 0.5° for α^{calc} (note that α^{calc} is normally 0.1° smaller than α^{pred}). The largest errors are observed for mean and individual A-O distances because these are extremely sensitive to the accuracy in the prediction of the tetrahedral rotation angle. An error of 0.5° in α^{pred} leads to an error of 0.008 Å in $\langle A-O \rangle_{in}$; increasing the error in α^{pred} up to 0.9° increases the error in $\langle A-O \rangle_{in}$ up to 0.026 Å. Table 4 compares selected basic structure parameters obtained from the calculated atomic coordinates with the observed values for natural samples of muscovite- $2M_1$ (numbers 12, 10, 6, 14), Mg-rich muscovite- $2M_1$ (no. 15), and phengite- $2M_1$ (numbers 18, 19), as well as

for synthetic aluminoceladonite 2M₁ (no. 20), for which the contents of tetrahedral Si and octahedral divalent cations pfhu vary from 3.03 to 3.81 and from 0.05 to 0.79, respectively. In Table 4, O-O_{oct,shared}, O-O_{oct,lateral}, and O-O_{oct,diagonal} stand for mean octahedral shared, unshared lateral and unshared diagonal edge lengths, respectively; *l_{apl}* is the elongated tetrahedral apical edge length (O1,2-O4) averaged over the two symmetrically independent tetrahedra; $\langle h_{\text{int}} \rangle$ is the mean interlayer distance. For most distance parameters except A-O, the discrepancies do not exceed 0.01 Å. In particular, close agreement is observed between the refined and modeled values for parameters that have not been predicted by regression equations, such as mean lateral, shared, and diagonal octahedral edge lengths. Larger discrepancies between the refined and modeled mean shared octahedral edge lengths (>0.2 Å) only occur for samples RA1 (no. 14 in Tables 1 and 4) and C3-31b (no. 13 in Table 1). The discrepancies of about 0.03 Å between the observed and modeled $\langle \text{A-O} \rangle_{\text{in}}$ and A-O4 distances for sample A4b (no. 12 in Tables 1 and 4) are associated with the relatively large error in *d_T* (0.007 Å), which leads to an overestimation of α^{calc} by 1.5°.

Note that in a few cases the experimental values in Table 4 differ from those given in the respective publications because the authors calculate them in the wrong way. For example, Ivaldi et al. (2001) and Gatta et al. (2011) calculate the mean interlayer

distance for 2M₁ structures as $\langle h_{\text{int}} \rangle = c \sin \beta / 2 - \langle h_{\text{oct}} \rangle - 2 \langle h_{\text{T}} \rangle$, i.e., used $\langle h_{\text{oct}} \rangle$ instead of $h_{\text{oct}}^{\text{max}}$. Similarly, Brigatti et al. (1998, 2001) calculate the mean tetrahedral sheet thickness as $(c \sin \beta / 2 - \langle h_{\text{oct}} \rangle - \langle h_{\text{int}} \rangle) / 2$. The resulting $\langle h_{\text{int}} \rangle$ and $\langle h_{\text{T}} \rangle$ values have no physical meaning. Therefore in such cases the corresponding values were recalculated from the published experimental unit-cell parameters and atomic coordinates.

As an independent test for the validity of the structure modeling procedure, atomic coordinates were calculated for three dioctahedral mica-2M₁ structures that were not included in the derivation of the empirical structure-composition relationships used in the algorithm: Fe-bearing muscovite-2M₁ (Gatta et al. 2011), muscovite-2M₁ (sample CC1b, Brigatti et al. 1998), and muscovite-2M₁ (Liang and Hawthorne 1996). The crystal-chemical formula for Fe-bearing muscovite-2M₁ (Gatta et al. 2011), K_{0.87}Na_{0.06}(Al_{1.7}Fe_{0.3}Mg_{0.02}Mn_{0.03}Ti_{0.02})(Si_{3.19}Al_{0.81})O₁₀(OH)₂, was calculated from the chemical analysis data in the original paper. All Fe was assumed divalent, as the sample was not analyzed for Fe valence. The composition of the sample is unusual in that it contains low Mg and high Fe. Among the structures included in regression analysis, only two muscovite samples (numbers 15 and 16, Table 1) have similar Fe contents. The calculated atomic coordinates, as well as the basic characteristics of the 2:1 layer and interlayer of the structure model, such as individual

TABLE 4. Comparison of selected basic structure parameters obtained from the calculated atomic coordinates (mod) with the observed (obs) values in refined structures of muscovite-, Mg-rich muscovite-, phengite-, and aluminoceladonite-2M₁ (sample numbers as in Table 1)

Sample no.	12		10		6		14		17		18		19		20	
Si (atoms pfhu)	2.92		3.03		3.11		3.18		3.25		3.38		3.45		3.81	
ΣR ²⁺ (atoms pfhu)	0.05		0.13		0.12		0.18		0.42		0.45		0.57		0.79	
parameter	obs	mod														
d(M-O, OH) (Å)	1.928	1.926	1.928	1.928	1.931	1.929	1.923	1.931	1.952	1.952	1.953	1.95	1.961	1.958	1.975	1.976
d(M-O) (Å)	1.936	1.931	1.934	1.934	1.934	1.936	1.933	1.938	1.958	1.959	1.963	1.959	1.97	1.968	1.986	1.988
O-O _{oct,lateral} (Å)	2.804	2.803	2.807	2.806	2.808	2.807	2.797	2.808	2.838	2.837	2.842	2.836	2.851	2.846	2.861	2.867
O-O _{oct,shared} (Å)	2.428	2.422	2.421	2.421	2.429	2.424	2.416	2.44	2.483	2.483	2.484	2.476	2.503	2.496	2.559	2.561
O-O _{oct,diagonal} (Å)	2.884	2.88	2.882	2.885	2.886	2.884	2.881	2.876	2.891	2.893	2.887	2.893	2.887	2.896	2.896	2.885
$\langle h_{\text{oct}} \rangle$ (Å)	2.095	2.089	2.086	2.09	2.095	2.092	2.088	2.096	2.121	2.122	2.118	2.12	2.13	2.131	2.164	2.159
d _{OH} (Å)	0.069	0.067	0.066	0.063	0.062	0.063	0.066	0.06	0.044	0.043	0.034	0.042	0.028	0.034	0.012	0.012
d _T (Å)	1.641	1.648	1.644	1.644	1.646	1.643	1.641	1.641	1.636	1.638	1.633	1.635	1.634	1.634	1.624	1.626
d _{nbr} (Å)	1.64	1.648	1.648	1.65	1.649	1.648	1.644	1.645	1.628	1.636	1.624	1.628	1.624	1.622	1.597	1.598
l _b (Å)	2.652	2.665	2.656	2.656	2.658	2.653	2.65	2.65	2.639	2.643	2.629	2.633	2.628	2.632	2.61	2.611
l _{bl} (Å)	2.684	2.695	2.69	2.686	2.687	2.682	2.684	2.676	2.666	2.664	2.649	2.656	2.648	2.649	2.626	2.623
l _{apl} (Å)	2.706	2.714	2.709	2.711	2.717	2.71	2.707	2.708	2.702	2.706	2.701	2.702	2.704	2.702	2.697	2.693
l _{apl} (Å)	2.723	2.73	2.727	2.731	2.734	2.728	2.728	2.72	2.719	2.73	2.72	2.726	2.722	2.727	2.704	2.707
$\langle h_{\text{T}} \rangle$ (Å)	2.218	2.223	2.221	2.223	2.229	2.223	2.223	2.22	2.222	2.225	2.226	2.225	2.229	2.225	2.22	2.226
ΔZ (Å)	0.218	0.222	0.218	0.217	0.216	0.214	0.216	0.214	0.183	0.175	0.171	0.175	0.161	0.161	0.133	0.128
α (°)	11.2	12.7	11.2	11.3	11.4	11	11.3	11.4	7.9	8.6	6.3	7	5.2	5.9	2.4	2.7
$\langle h_{\text{int}} \rangle$ (Å)	3.385	3.384	3.404	3.399	3.37	3.384	3.379	3.368	3.342	3.336	3.325	3.321	3.321	3.324	3.288	3.276
$\langle \text{A-O} \rangle$ (Å)	2.854	2.823	2.863	2.861	2.848	2.864	2.849	2.846	2.924	2.906	2.957	2.94	2.983	2.965	3.029	3.019
A-O4 (Å)	2.87	2.844	2.882	2.882	2.867	2.885	2.869	2.866	2.948	2.929	2.948	2.933	3.005	2.986	3.055	3.041

* ΣR²⁺ = sum of divalent octahedral cations pfhu.

TABLE 5. Comparison of fractional atomic coordinates in the refined structure of Fe-rich muscovite K_{0.87}Na_{0.06}(Al_{1.7}Fe_{0.3}Mg_{0.02}Mn_{0.03}Ti_{0.02})(Si_{3.19}Al_{0.81})O₁₀(OH)₂, *a* = 5.2093(2) Å, *b* = 9.0390(4) Å, *c* = 20.034(7) Å, β = 95.782(2)° (Gatta et al. 2011) and in the structure model based on the crystal-chemical formula and unit-cell parameters (A = interlayer cation site; T1, T2 = tetrahedral cation sites; M = occupied octahedral site; O1, O2 = apical oxygen anion sites; OH = hydroxyl oxygen anion site; O3, O4, O5 = basal oxygen anion sites)

Atom	x		y		z	
	Structure refinement (Gatta et al. 2011)	Structure model (this study)	Structure refinement (Gatta et al. 2011)	Structure model (this study)	Structure refinement (Gatta et al. 2011)	Structure model (this study)
A	0	0	0.0977(5)	0.097(1)	0.25	0.25
M	0.2502(3)	0.2486(7)	0.0833(2)	0.0831(2)	-0.0001(1)	0.0000(1)
T1	0.9645(3)	0.9649(8)	0.4293(2)	0.430(1)	0.1356(1)	0.1360(2)
T2	0.4518(3)	0.453(1)	0.2582(2)	0.259(1)	0.1355(1)	0.1360(2)
O1	0.4594(2)	0.460(2)	-0.0584(2)	-0.058(1)	0.0536(1)	0.0539(3)
O2	0.3891(2)	0.389(2)	0.2513(2)	0.2511(4)	0.0536(1)	0.0539(2)
O3	0.4256(2)	0.427(3)	0.0930(2)	0.093(1)	0.1685(1)	0.1686(2)
O4	0.7450(3)	0.746(2)	0.3159(2)	0.316(2)	0.1588(1)	0.1592(3)
O5	0.2449(3)	0.245(3)	0.3659(2)	0.366(1)	0.1687(1)	0.1686(3)
OH	0.9559(3)	0.956(1)	0.0639(2)	0.0637(9)	0.0510(1)	0.0512(3)

interatomic distances, tetrahedral, and octahedral sheet thicknesses and basal surface corrugations, interlayer distances and tetrahedral rotation angle, agree well with the corresponding observed parameters (Tables 5 and 6). The discrepancies between the modeled and observed values for individual bond and edge lengths, and sheet thicknesses and corrugations are 0.002–0.010

Å (Table 6). The significant underestimation of the *x* coordinate of the octahedral cation (0.0016 fractional units, Table 5) corresponds with the relatively low significance level of Equation 6a and may indicate that either the effect of Fe²⁺ on *x*_M is weaker than that of Mg or the actual Fe²⁺ content is lower than reported, and some of the Fe cations are trivalent. This discrepancy, how-

TABLE 6. Comparison of interatomic distances (Å) and selected octahedral, tetrahedral and interlayer parameters in the refined structure of Fe-rich muscovite (Gatta et al. 2011) and in the structure model based on the crystal-chemical formula and unit-cell parameters

	Structure refinement*	Structure model†		Structure refinement*	Structure model†
T1-O1	1.644	1.646	M-O1	1.954	1.962
-O3	1.641	1.637	-O1'	1.936	1.942
-O4	1.638	1.634	-O2	1.938	1.942
-O5	1.645	1.634	-O2'	1.957	1.962
mean	1.642	1.640	-OH	1.935	1.930
O1-O3	2.699	2.695	-OH'	1.935	1.930
-O4	2.730	2.730	mean	1.945	1.945
-O5	2.703	2.696	O1-O2	2.823	2.822
mean					
apical	2.711	2.707	O1-OH	2.818	2.813
O3-O4	2.676	2.675	O2-OH	2.848	2.848
O3-O5	2.642	2.641	O1'-O2'	2.823	2.820
O4-O5	2.631	2.624	O1'-OH'	2.842	2.844
mean					
basal	2.650	2.647	O2'-OH'	2.818	2.818
T2-O2	1.641	1.646	mean		
lateral	2.829	2.827			
-O3	1.641	1.643	O1-O1'	2.468	2.475
-O4	1.637	1.635	O2-O2'	2.467	2.476
-O5	1.642	1.636	OH-OH'	2.423	2.437
mean	1.641	1.640	mean		
shared	2.455	2.463			
O2-O3	2.701	2.695	O1-O2'	2.935	2.944
-O4	2.726	2.732	O2-OH'	2.859	2.869
-O5	2.702	2.695	O1'-OH	2.857	2.865
mean					
apical	2.710	2.707	mean		
diagonal	2.884	2.893			
O3-O4	2.633	2.630	A-O3 _{inner}	2.883	2.889
O3-O5	2.640	2.638	A-O4 _{inner}	2.916	2.920
O4-O5	2.671	2.673	A-O5 _{inner}	2.893	2.890
mean					
basal	2.648	2.647	mean		
inner	2.897	2.900			
<h _{oct} >, Å	2.103	2.112	α, °	9.5	9.4
Δ _{OH} , Å	0.052	0.054	ΔZ, Å	0.195	0.187
<h _T >, Å	2.227	2.224	<h _{int} >, Å	3.375	3.370

* Gatta et al. (2011).

† This study.

TABLE 8. Comparison of interatomic distances (Å) and selected octahedral, tetrahedral, and interlayer parameters in the refined structure of muscovite-2M₁ (sample CC1b) (Brigatti et al. 1998) and in the structure model based on the crystal-chemical formula and unit-cell parameters

	Structure refinement*	Structure model†		Structure refinement*	Structure model†
T1-O1	1.646	1.647	M-O1	1.944	1.945
-O3	1.640	1.635	-O1'	1.924	1.925
-O4	1.634	1.635	-O2	1.926	1.926
-O5	1.647	1.642	-O2'	1.947	1.945
mean	1.642	1.640	-OH	1.910	1.914
O1-O3	2.696	2.701	-OH'	1.911	1.913
-O4	2.726	2.722	mean	1.927	1.928
-O5	2.705	2.699	O1-O2	2.797	2.799
mean					
apical	2.709	2.707	O1-OH	2.791	2.797
O3-O4	2.682	2.678	O2-OH	2.823	2.821
O3-O5	2.644	2.638	O1'-O2'	2.801	2.804
O4-O5	2.629	2.623	O1'-OH'	2.819	2.815
mean					
basal	2.652	2.646	O2'-OH'	2.796	2.796
T2-O2	1.644	1.648	mean		
lateral	2.804	2.805			
-O3	1.643	1.643	O1-O1'	2.440	2.448
-O4	1.639	1.635	O2-O2'	2.441	2.442
-O5	1.642	1.635	OH-OH'	2.383	2.384
mean	1.642	1.640	mean		
shared	2.421	2.425			
O2-O3	2.696	2.700	O1-O2'	2.938	2.938
-O4	2.727	2.724	O2-OH'	2.857	2.858
-O5	2.702	2.700	O1'-OH	2.849	2.851
mean					
apical	2.708	2.708	mean		
diagonal	2.881	2.882			
O3-O4	2.642	2.637	A-O3 _{inner}	2.846	2.853
O3-O5	2.638	2.630	A-O4 _{inner}	2.879	2.893
O4-O5	2.681	2.676	A-O5 _{inner}	2.855	2.871
mean					
basal	2.654	2.648	mean		
inner	2.860	2.872			
<h _{oct} >, Å	2.090	2.091	α, °	11.1	10.6
Δ _{OH} , Å	0.063	0.062	ΔZ, Å	0.216	0.215
<h _T >, Å	2.222	2.222	<h _{int} >, Å	3.391	3.388

* Brigatti et al. (1998).

† This study.

TABLE 7. Comparison of fractional atomic coordinates in the refined structure of muscovite-2M₁ (sample CC1b) K_{0.93}Na_{0.07}(Al_{1.83}Fe_{0.07}Mg_{0.07}Ti_{0.06})(Si_{3.18}Al_{0.82})O_{10.21}(OH)_{1.79}, *a* = 5.186(1), *b* = 9.005(4), *c* = 20.031(3) Å, β = 95.78(1)° (Brigatti et al. 1998) and in the structure model based on the crystal-chemical formula and unit-cell parameters

Atom	<i>x</i>		<i>y</i>		<i>z</i>	
	Structure refinement*	Structure model†	Structure refinement*	Structure model†	Structure refinement*	Structure model†
A	0	0	0.09858(8)	0.099(1)	0.25	0.25
M	0.2491(1)	0.2498(7)	0.08314(6)	0.0833(2)	0.00002(3)	0.0000(1)
T1	0.96505(9)	0.9646(8)	0.42957(5)	0.430(1)	0.13548(2)	0.1356(2)
T2	0.45162(9)	0.451(1)	0.25835(5)	0.259(1)	0.13546(2)	0.1356(2)
O1	0.4613(2)	0.461(2)	-0.0567(1)	-0.057(1)	0.05344(6)	0.0535(3)
O2	0.3854(2)	0.386(2)	0.2513(1)	0.2513(4)	0.05351(6)	0.0535(2)
O3	0.4180(3)	0.421(3)	0.0930(2)	0.093(1)	0.16826(7)	0.1686(2)
O4	0.7503(3)	0.749(2)	0.3114(2)	0.313(2)	0.15768(7)	0.1578(3)
O5	0.2494(3)	0.247(3)	0.3698(2)	0.368(1)	0.16880(7)	0.1686(3)
OH	0.9572(2)	0.958(1)	0.0619(1)	0.0617(9)	0.05034(6)	0.0504(3)

Note: A = interlayer cation site; T1, T2 = tetrahedral cation sites; M = occupied octahedral site; O1, O2 = apical oxygen anion sites; OH = hydroxyl oxygen anion site; O3, O4, O5 = basal oxygen anion sites.

* Brigatti et al. (1998).

† This study.

ever, does not affect significantly the agreement between other modeled and observed structure characteristics.

Sample CC1b, $K_{0.93}Na_{0.07}(Al_{1.83}Fe_{0.07}Mg_{0.07}Ti_{0.06})(Si_{3.18}Al_{0.82})O_{10.21}(OH)_{1.79}$ (Brigatti et al. 1998), was not included in the regression analysis because its overall cation charge *phfu* is >22.15. Nevertheless the calculated atomic coordinates, interatomic distances and other characteristics of the 2:1 layer and interlayer are in close agreement with the observed parameters in the refined structure (Tables 7 and 8). The discrepancies between the modeled and observed individual tetrahedral and octahedral bond and edge lengths are 0.001–0.008 Å; for sheet thicknesses

and surface corrugations, the discrepancies are 0.001–0.003 Å (Table 8). The underestimation of the tetrahedral rotation angle by 0.5° resulted in the overestimation of the individual interlayer cation-oxygen inner distances by 0.007–0.016 Å (the mean *A*-*O*_{inner} distance is overestimated by 0.012 Å).

Liang and Hawthorne (1996) refined the structure of muscovite-2M₁, $K_{0.876}Na_{0.096}Rb_{0.01}(Al_{1.954}Fe_{0.029}Mg_{0.013})(Si_{3.068}Al_{0.932})O_{10}(OH)_{1.744}F_{0.256}$, by single-crystal X-ray diffraction and by the Rietveld method using X-ray powder diffraction data, which allowed us to compare the results of structure modeling with both structure refinement techniques. Although the sample

TABLE 9. Comparison of fractional atomic coordinates of muscovite-2M₁ $K_{0.876}Na_{0.096}Rb_{0.01}(Al_{1.954}Fe_{0.029}Mg_{0.013})(Si_{3.068}Al_{0.932})O_{10}(OH)_{1.744}F_{0.256}$, obtained by single-crystal and Rietveld structure refinement (Liang and Hawthorne 1996), and by structure modeling (this study) based on the crystal-chemical formula and unit-cell parameters

Atom	x			y			z		
	Single-crystal refinement	Structure model	Rietveld refinement	Single-crystal refinement	Structure model	Rietveld refinement	Single-crystal refinement	Structure model	Rietveld refinement
A	0	0	0	0.0986(2)	0.100(1)	0.104(1)	0.25	0.25	0.25
M	0.2510(2)	0.2504(7)	0.249(2)	0.0838(2)	0.0835(2)	0.081(1)	0.0000(1)	0.0000(1)	-0.0012(5)
T1	0.9655(2)	0.9640(8)	0.968(2)	0.4295(1)	0.431(1)	0.428(1)	0.1354(1)	0.1353(2)	0.1358(4)
T2	0.4514(2)	0.450(1)	0.447(2)	0.2582(1)	0.259(1)	0.256(1)	0.1355(1)	0.1353(2)	0.1346(4)
O1	0.4620(6)	0.461(2)	0.465(2)	-0.0553(3)	-0.056(1)	-0.058(2)	0.0537(2)	0.0533(3)	0.0517(8)
O2	0.3836(6)	0.384(2)	0.379(3)	0.2511(3)	0.2515(4)	0.246(2)	0.0536(2)	0.0533(2)	0.0540(8)
O3	0.4128(6)	0.414(3)	0.413(3)	0.0925(4)	0.094(1)	0.090(3)	0.1682(2)	0.1684(2)	0.1667(6)
O4	0.7531(7)	0.750(2)	0.752(4)	0.3083(4)	0.310(2)	0.307(2)	0.1574(2)	0.1570(3)	0.1562(7)
O5	0.2516(6)	0.249(3)	0.257(4)	0.3726(4)	0.372(1)	0.372(2)	0.1688(2)	0.1684(3)	0.1691(6)
OH	0.9571(6)	0.957(1)	0.955(3)	0.0617(3)	0.0614(9)	0.068(2)	0.0499(2)	0.0498(3)	0.0474(8)

Notes: A = interlayer cation site; T1, T2 = tetrahedral cation sites; M = occupied octahedral site; O1, O2 = apical oxygen anion sites; OH = hydroxyl oxygen anion site; O3, O4, O5 = basal oxygen anion sites. Unit-cell parameters: single-crystal refinement and structure model, $a = 5.180(4)$, $b = 8.993(6)$, $c = 20.069(13)$ Å, $\beta = 95.69(8)^\circ$; Rietveld refinement, $a = 5.1805(7)$, $b = 8.994(1)$, $c = 20.086(13)$ Å, and $\beta = 95.69(8)^\circ$.

TABLE 10. Comparison of interatomic distances (Å) and selected octahedral, tetrahedral and interlayer parameters in the structure of muscovite-2M₁, obtained from single-crystal and Rietveld refinements (Liang and Hawthorne 1996), and those in the structure model based on the crystal-chemical formula and unit-cell parameters (this study)

	Single-crystal refinement	Structure model	Rietveld refinement		Single-crystal refinement	Structure model	Rietveld refinement
T1-O1	1.643	1.649	1.69	M-O1	1.938	1.938	1.89
-O3	1.642	1.639	1.62	-O1'	1.920	1.919	1.93
-O4	1.641	1.640	1.64	-O2	1.924	1.919	1.97
-O5	1.646	1.645	1.65	-O2'	1.936	1.938	1.93
mean	1.643	1.643	1.65	-OH	1.913	1.908	1.89
O1-O3	2.689	2.706	2.70	-OH'	1.913	1.909	1.89
-O4	2.730	2.724	2.75	mean	1.924	1.922	1.92
-O5	2.705	2.701	2.74	O1-O2	2.794	2.791	2.77
mean							
apical	2.708	2.710	2.73	O1-OH	2.780	2.788	2.79
O3-O4	2.688	2.689	2.68	O2-OH	2.821	2.815	2.93
O3-O5	2.643	2.645	2.65	O1'-O2'	2.785	2.796	2.77
O4-O5	2.634	2.631	2.67	O1'-OH'	2.813	2.809	2.87
mean							
basal	2.655	2.655	2.67	O2'-OH'	2.786	2.788	2.71
T2-O2	1.646	1.649	1.62	mean			
lateral	2.796	2.798	2.81				
-O3	1.650	1.646	1.64	O1-O1'	2.441	2.436	2.38
-O4	1.643	1.639	1.66	O2-O2'	2.441	2.431	2.43
-O5	1.649	1.639	1.64	OH-OH'	2.370	2.363	2.35
mean	1.647	1.643	1.64	mean			
shared	2.417	2.410	2.39				
O2-O3	2.698	2.702	2.65	O1-O2'	2.952	2.941	2.89
-O4	2.734	2.725	2.73	O2-OH'	2.858	2.851	2.83
-O5	2.706	2.704	2.71	O1'-OH	2.854	2.845	2.80
mean							
apical	2.713	2.710	2.70	mean			
diagonal	2.888	2.879	2.84				
O3-O4	2.645	2.638	2.65	A-O3 _{inner}	2.824	2.825	2.85
O3-O5	2.654	2.643	2.66	A-O4 _{inner}	2.860	2.873	2.84
O4-O5	2.693	2.686	2.67	A-O5 _{inner}	2.833	2.857	2.86
mean							
basal	2.664	2.656	2.65	mean			
inner	2.839	2.851	2.85				
$\langle h_{oct} \rangle$, Å	2.093	2.083	2.040	α , °	12.2	11.8	12
Δ_{OH} , Å	0.075	0.070	0.108	ΔZ , Å	0.222	0.227	0.234
$\langle h_T \rangle$, Å	2.220	2.222	2.221	$\langle h_{int} \rangle$, Å	3.403	3.410	3.437

contains 0.256 F anions pfu, the calculated atomic coordinates, interatomic distances, tetrahedral and octahedral sheet thicknesses, and basal surface corrugations, interlayer distances, and tetrahedral rotation angle in the structure model agree well with those obtained by single-crystal structure refinement (Tables 9 and 10). The discrepancies between the modeled and observed tetrahedral and octahedral interatomic distances, sheet thicknesses and corrugations are 0–0.011 Å, with the exception of the O1–O3 tetrahedral edge length, which is overestimated by 0.017 Å. The structure modeling algorithm is insensitive to possible cation ordering, and therefore failed to reproduce the slight tendency to ordering between the T1 and T2 sites (T1–O1 = 1.643 Å; T2–O2 = 1.647 Å); at the same time, the modeled mean tetrahedral bond length agrees well with the corresponding observed value averaged over the two tetrahedral sites (1.643 and 1.645 Å, respectively). The mean interlayer cation–oxygen inner distance and the individual A–O4 and A–O5 distances are overestimated by 0.012, 0.013, and 0.024 Å, respectively, because of the underestimation of α by 0.4° (Table 10).

As compared with the Rietveld refinement, the structure modeling procedure provided better agreement with the fractional atomic coordinates obtained by single-crystal refinement for all the z coordinates, the x coordinates of the M and T1 sites, and the y coordinates of the M and O2 sites; for the rest of the atomic sites, structure modeling and Rietveld refinement showed similar degree of agreement in fractional coordinates (Table 9). For the majority of structure parameters in Table 10, the degree of agreement between the modeled values and those obtained by single-crystal refinement is much higher than that ensured by the Rietveld refinement. Indeed, quite a few Rietveld-refined individual bond and edge lengths, as well as sheet thicknesses differ dramatically from the corresponding single-crystal-refined parameters: for octahedral bond and edge lengths the discrepancies reach 0.05–0.1 Å; for mean octahedral sheet thickness, the octahedral basal surface corrugation, and the mean interlayer distance, the discrepancies are 0.053, 0.033, and 0.034 Å, respectively. The Rietveld method and structure modeling provide similar degree of agreement for some of the individual and mean tetrahedral bond and edge lengths around T2, for the mean octahedral bond length, the O2–O2' shared octahedral edge length, the A–O5 and mean interlayer distances, mean tetrahedral sheet thickness, and α . The only parameter, for which better agreement is obtained by the Rietveld refinement, is the O1–O3 edge length (Table 10). On the whole, the structure modeling algorithm reproduces the fine structural features of the muscovite in question better than the Rietveld refinement.

To conclude, K-dioctahedral micas- $2M_1$ (space group $C2/c$) having disordered cation distribution can be modeled from the data on the unit-cell parameters and cation composition, and the structure modeling algorithm can be used as a simple, cheap, and express method for reliable evaluation of fine structural features in large collections of mica samples, where direct experimental structure determinations would be more expensive and time consuming.

ACKNOWLEDGMENTS

The authors are grateful to Douglas McCarty and Sonia Schatzman for help and valuable discussion. The work was supported by Russian Foundation for Basic Research (RFBR grant 12-05-00381).

REFERENCES CITED

- Appelo, C.A. (1978) Layer deformation and crystal energy of micas and related minerals. I. Structural models for $1M$ and $2M_1$ polytypes. *American Mineralogist*, 63, 782–792.
- Bailey, S.W. (1984) Crystal chemistry of the true mica. In S.W. Bailey, Ed., *Micas*, 13, 13–66. *Reviews in Mineralogy*, Mineralogical Society of America, Chantilly, Virginia.
- Baur, W.H. (1981) Interatomic distance prediction for computer simulation of crystal structures. In M. O'Keefe and A. Navrotsky, Eds., *Structure and Bonding in Crystals*, 31–52. Academic Press, New York.
- Bookin, A.S. and Smoliar, B.B. (1985) Simulation of bondlengths in coordination polyhedra of 2:1 layer silicates. In J. Konta, Ed., *Proceedings of the 5th Meeting of the European Clay Groups*, p. 51–56, Univerzita Karlova, Prague.
- Brigatti, M.F. and Guggenheim, S. (2002) Mica crystal chemistry and the influence of pressure, temperature and solid solution on atomistic models. In A. Mottana, F.E. Sassi, J.B. Thompson Jr., and S. Guggenheim, Eds., *Micas: Crystal chemistry and metamorphic petrology*, 46, p. 1–97. *Reviews in Mineralogy and Geochemistry*, Mineralogical Society of America, Chantilly, Virginia, with Accademia Nazionale dei lincei, Roma, Italy.
- Brigatti, M.F., Frigieri, P., and Poppi, L. (1998) Crystal chemistry of Mg-, Fe²⁺-bearing muscovites- $2M_1$. *American Mineralogist*, 83, 775–785.
- Brigatti, M.F., Galli, E., Medici, L., Poppi, L., Cibin, G., Marcelli, A., and Mottana, A. (2001) Chromium-containing muscovite: crystal chemistry and XANES spectroscopy. *European Journal of Mineralogy*, 13, 377–389.
- Brigatti, M.F., Guggenheim, S., and Poppi, M. (2003) Crystal chemistry of the $1M$ mica polytype: The octahedral sheet. *American Mineralogist*, 88, 667–675.
- Brigatti, M.F., Malferrari, D., Poppi, M., and Poppi, L. (2005) The $2M_1$ dioctahedral mica polytype: a crystal-chemical study. *Clays and Clay Minerals*, 53, 190–197.
- Brigatti, M.F., Malferrari, D., Poppi, M., Mottana, A., Cibin, G., Marcelle, A., and Cinque, G. (2008) Interlayer potassium and its neighboring atoms in micas: Crystal-chemical modeling and XANES spectroscopy. *American Mineralogist*, 93, 821–830.
- Comodi, P. and Zanazzi, P.F. (1997) Pressure dependence of structural parameters of paragonite. *Physics and Chemistry of Minerals*, 24, 274–280.
- (2000) Structural thermal behavior of paragonite and its dehydroxylate: a high-temperature single-crystal study. *Physics and Chemistry of Minerals*, 27, 377–385.
- Donnay, G., Donnay, J.D.H., and Takeda, H. (1964) Trioctahedral one-layer micas. II. Prediction of the structure from composition and cell dimensions. *Acta Crystallographica*, 17, 1374–1381.
- Drits, V.A. (1969) Some remarks on the structure of trioctahedral micas. *Proceedings of the 4th International Clay Conference*, Tokyo, 1, 51–59.
- (1975) Structural and crystal-chemical features of layer silicates. In A.G. Kossovskaya, Ed., *Kristalloghimiya mineralov i geologicheskoye problemy*, 35–51. Nauka, Moscow (in Russian).
- Drits, V.A. and Kossovskaya, A.G. (1991) *Clay Minerals: Micas and Chlorites*, 175 p. Nauka, Moscow (in Russian).
- Drits, V.A. and Zviagina, B.B. (2009) *Trans*-vacant and *cis*-vacant 2:1 layer silicates: structural features, identification and occurrence. *Clays and Clay Minerals*, 57, 405–415.
- Drits, V.A., Tsipursky, S., and Plançon, A. (1984) Application of the method for the calculation of intensity distribution to electron diffraction structure analysis. *Izvestiya Akademii Nauk SSSR, Seriya Fizicheskaya*, 2, 1708–1713 (in Russian).
- Drits, V.A., McCarty, D.K., and Zviagina, B.B. (2006) Crystal-chemical factors responsible for the distribution of octahedral cations over *trans*- and *cis*-sites in dioctahedral 2:1 layer silicates. *Clays and Clay Minerals*, 54, 131–153.
- Drits, V.A., Zviagina, B.B., McCarty, D.K., and Salyn, A.L. (2010) Factors responsible for crystal-chemical variations in the solid solutions from illite to aluminoceladonite and from glauconite to celadonite. *American Mineralogist*, 95, 348–361.
- Ferraris, G. and Ivaldi, G. (2002) Structural features of micas. In A. Mottana, F.E. Sassi, J.B. Thompson Jr., and S. Guggenheim, Eds., *Micas: Crystal Chemistry and Metamorphic Petrology*, 46, p. 117–153. *Reviews in Mineralogy and Geochemistry*, Mineralogical Society of America, Chantilly, Virginia, with Accademia Nazionale dei lincei, Roma, Italy.
- Franzini, M. and Schiaffino, L. (1963) On the crystal structures of biotites. *Zeitschrift für Kristallographie*, 119, 297–309.
- Gatta, G.D., McIntyre, G.J., Sassi, R., Rotiroli, N., and Pavese, A. (2011) Hydrogen-bond and cation partitioning in muscovite: A single-crystal neutron-diffraction study at 295 and 20 K. *American Mineralogist*, 96, 34–41.
- Guggenheim, S. and Bailey, S.W. (1978) Refinement of the margarite structure in subgroup symmetry: correction, further refinement, and comments. *American Mineralogist*, 63, 186–187.
- Guggenheim, S., Chang, Y.H., and Koster van Groos, A.F. (1987) Muscovite dehydroxylation: High-temperature studies. *American Mineralogist*, 72, 537–550.
- Güven, N. (1971) The crystal structures of $2M_1$ phengite and $2M_1$ muscovite. *Zeitschrift für Kristallographie*, 134, 196–212.
- Hazen, R.M. and Burnham, C.W. (1973) The crystal structures of one-layer phlogopite and annite. *American Mineralogist*, 58, 889–900.
- Hazen, R.M. and Wones, D.R. (1972) The effect of cation substitutions on the physical properties of trioctahedral micas. *American Mineralogist*, 57, 103–129.
- (1978) Predicted and observed compositional limits of trioctahedral micas. *American Mineralogist*, 63, 885–892.

Ivaldi, G., Ferraris, G., Curetti, N., and Compagnoni, R. (2001) Coexisting 3T and 2M₁ polytypes of phengite from Cima Pal (Val Savenca, western Alps): Chemical and polytypic zoning and structural characterization. *European Journal of Mineralogy*, 13, 1025–1034.

Joswig, W., Takéuchi, Y., and Fuess, H. (1983) Neutron-diffraction study on the orientation of hydroxyl groups in margarite. *Zeitschrift für Kristallographie*, 165, 295–303.

Knurr, R.A. and Bailey, S.W. (1986) Refinement of Mn-substituted muscovite and phlogopite. *Clays and Clay Minerals*, 34, 7–16.

Li, G., Peacor, D.R., Coombs, D.S., and Kawachi, Y. (1997) Solid solution in the celadonite family: The new minerals ferroccladonite K₂Fe²⁺Fe³⁺Si₆O₂₀(OH)₄ and ferroaluminoccladonite K₂Fe²⁺Al₂Si₆O₂₀(OH)₄. *American Mineralogist*, 82, 503–511.

Liang, J.-J. and Hawthorne, F.C. (1996) Rietveld refinement of micaceous materials: muscovite-2M₁, a comparison with single-crystal structure refinement. *Canadian Mineralogist*, 34, 115–122.

Lin, C.Y. and Bailey, S.W. (1984) The crystal structure of paragonite-2M₁. *American Mineralogist*, 69, 122–127.

Lin, J.-C. and Guggenheim, S. (1983) The crystal structure of Li, Be-rich brittle mica: a dioctahedral-trioctahedral intermediate. *American Mineralogist*, 68, 130–142.

McCauley, J.M. and Newham, R.E. (1971) Origin and prediction of ditrigonal distortions in micas. *American Mineralogist*, 56, 1626–1638.

Mercier, P.H.J., Evans, R.J., and Rancourt, D.G. (2005) Geometric crystal chemical models for structural analysis of micas and their stacking polytypes. *American Mineralogist*, 90, 382–398.

Mercier, P.H.J., Rancourt, D.G., Redhammer, G.J., Lalonde, A.E., Robert, J.-L., Berman, R.G., and Kodama, H. (2006) Upper limit of the tetrahedral rotation angle and factors affecting octahedral flattening in synthetic and natural 1M polytype C2/m space group micas. *American Mineralogist*, 91, 831–849.

Pauling, L. (1930) The structure of micas and related minerals. *Proceedings of the National Academy of Sciences*, 16, 123–129.

Pavese, A., Ferraris, G., Pischedda, V., and Ibberson, R. (1999) Tetrahedral order in phengite 2M₁ upon heating, from powder neutron diffraction, and thermodynamic consequences. *European Journal of Mineralogy*, 11, 309–320.

Radoslovich, E.W. (1961) Surface symmetry and cell dimensions of layer-lattice silicates. *Nature*, 191, 67–68.

——— (1962) The cell dimensions and symmetry of layer-lattice silicates. II. Regression relations. *American Mineralogist*, 47, 599–616.

Redhammer, G.J. and Roth, G. (2002) Single-crystal structure refinements and crystal chemistry of synthetic trioctahedral micas KM₃(Al³⁺, Si⁴⁺)₆O₁₀(OH)₂, where M = Ni²⁺, Mg²⁺, Co²⁺, Fe²⁺, or Al³⁺. *American Mineralogist*, 87, 1464–1476.

Rieder, M., Cavazzini, G., Dyakonov, Y.S., Frank-Kamenetskii, V.A., Gottardi, G., Guggenheim, S., Koval, P.V., Müller, G., Neiva, A.M.R., Radoslovich, E.W., and others (1998) Nomenclature of the micas. *Clays and Clay Minerals*, 46, 586–595.

Rothbauer, von R. (1971) Untersuchung eines 2M₁-muskovits mit neutronenstrahlen. *Neues Jahrbuch für Mineralogie Monatshefte*, 143–154.

Rule, A.C. and Bailey, S.W. (1985) Refinement of the crystal structure of phengite-2M₁. *Clays and Clay Minerals*, 33, 403–409.

Schmidt, M.W., Dugnani, M., and Artioli, G. (2001) Synthesis and characterization of white micas in the joint muscovite-aluminoccladonite. *American Mineralogist*, 86, 555–565.

Smoliar-Zviagina, B.B. (1993) Relationships between structural parameters and chemical composition of micas. *Clay Minerals*, 25, 603–624.

Smyth, J.R., Jacobsen, S.D., Swope, R.J., Angel, R.J., Arlt, T., Domanik, K., and Holloway, J.R. (2000) Crystal structures and compressibilities of synthetic 2M₁ and 3T phengite micas. *European Journal of Mineralogy*, 12, 955–963.

Šrodoň, J. and Eberl, D.D. (1984) Illite. In S.W. Bailey, Ed., *Micas*, 13, p. 495–544. *Reviews in Mineralogy*, Mineralogical Society of America, Chantilly, Virginia.

Takeda, H. and Morosin, B. (1975) Comparison of observed and predicted structural parameters of mica at high temperature. *Acta Crystallographica B*, 31, 2444–2452.

Tepikin, E.V., Drits, V.A., and Alexandrova, V.A. (1969) Crystal structure of iron biotite and construction of structural models for trioctahedral micas. *Proceedings of the 4th International Clay Conference*, Tokyo, 1, 43–49.

Toraya, H. (1981) Distortions of octahedra and octahedral sheets in 1M micas and the relation to their stability. *Zeitschrift für Kristallographie*, 157, 173–190.

Tsipursky, S.I. and Drits, V.A. (1977) Effectivity of the electronic method of intensity measurement in structural investigation by electron diffraction. *Izvestija Akademii Nauk SSSR, Serija fiziko-matematicheskaja*, 41, 2263–2271 (in Russian).

Weiss, Z., Rieder, M., Chmielova, M., and Krajčiek, J. (1985) Geometry of the octahedral coordination in micas: a review of refined structures. *American Mineralogist*, 70, 747–757.

Weiss, Z., Rieder, M., and Chmielova, M. (1992) Deformation of coordination polyhedra and their sheets in phyllosilicates. *European Journal of Mineralogy*, 4, 665–682.

Zhoukhlisov, A.P. (2005) Crystal structure of celadonite from electron diffraction data. *Crystallography Reports*, 50, 902–906 (translated from *Kristallografiya*, 50, 976–980).

APPENDIX TABLE 1. Comparison of the refined and modeled fractional atomic coordinates for K-dioctahedral micas-2M₁ (sample numbers as in Table 1; the monoclinic fractional coordinates, *x*, *y*, *z*, are related to Cartesian coordinates *X*, *Y*, *Z* (Å), as $x = (1/a)(X - Z/\tan\beta)$; $y = Y/b$; $z = Z/c\sin\beta$)

	x		y		z	
	obs	mod	obs	mod	obs	mod
1						
K	0	0	0.098	0.099(1)	0.25	0.25
M	0.2498	0.2497(7)	0.0835	0.0833(2)	0.0000	0.0000(1)
T1	0.9646	0.9641(8)	0.4291	0.431(1)	0.1355	0.1356(2)
T2	0.4516	0.451(1)	0.2581	0.259(1)	0.1356	0.1356(2)
O1	0.4610	0.461(2)	-0.0568	-0.057(1)	0.0534	0.0535(3)
O2	0.3859	0.385(2)	0.2515	0.2513(4)	0.0535	0.0535(2)
OH	0.4556	0.457(1)	0.5627	0.5619(9)	0.0502	0.0503(3)
O3	0.4167	0.419(3)	0.0927	0.094(1)	0.1683	0.1685(2)
O4	0.7505	0.748(2)	0.3107	0.313(2)	0.1578	0.1578(3)
O5	0.2502	0.247(2)	0.3703	0.369(1)	0.1687	0.1685(3)
2						
K	0	0	0.0988	0.098(1)	0.25	0.25
M	0.2498	0.2502(7)	0.0832	0.0833(2)	0.0000	0.0000(1)
T1	0.9650	0.9655(8)	0.4299	0.430(1)	0.1355	0.1357(2)
T2	0.4514	0.452(1)	0.2587	0.259(1)	0.1356	0.1357(2)
O1	0.4616	0.460(2)	-0.0563	-0.057(1)	0.0537	0.0536(3)
O2	0.3833	0.386(2)	0.2518	0.2514(4)	0.0537	0.0536(2)
OH	0.4576	0.458(1)	0.5621	0.5621(9)	0.0508	0.0504(3)
O3	0.4195	0.419(3)	0.0933	0.093(1)	0.1685	0.1684(2)
O4	0.7489	0.750(2)	0.3126	0.312(2)	0.1577	0.1580(3)
O5	0.2484	0.250(2)	0.3692	0.370(1)	0.1689	0.1684(3)
3						
K	0	0	0.0991	0.099(1)	0.25	0.25
M	0.2506	0.2500(7)	0.0834	0.0833(2)	0.0002	0.0000(1)
T1	0.9661	0.9649(8)	0.4289	0.429(1)	0.1356	0.1356(2)
T2	0.4516	0.452(1)	0.2581	0.258(1)	0.1356	0.1356(2)
O1	0.4615	0.460(2)	-0.0553	-0.057(1)	0.0534	0.0535(3)
O2	0.3869	0.386(2)	0.2523	0.2514(4)	0.0538	0.0535(2)
OH	0.4585	0.458(1)	0.5614	0.5618(9)	0.0502	0.0504(3)
O3	0.4193	0.418(3)	0.0926	0.093(1)	0.168	0.1685(2)
O4	0.7526	0.749(2)	0.3107	0.312(2)	0.157	0.1578(3)
O5	0.2499	0.249(2)	0.3705	0.370(1)	0.1688	0.1685(3)
4						
K	0	0	0.0985	0.099(1)	0.25	0.25
M	0.2496	0.2500(7)	0.0834	0.0834(2)	-0.0001	0.0000(1)
T1	0.9648	0.9646(8)	0.4295	0.430(1)	0.1355	0.1355(2)
T2	0.4510	0.451(1)	0.2584	0.259(1)	0.1355	0.1355(2)
O1	0.4613	0.461(2)	-0.0565	-0.056(1)	0.054	0.0534(3)
O2	0.3850	0.384(2)	0.2519	0.2514(4)	0.0537	0.0534(2)
OH	0.4564	0.457(1)	0.5630	0.5619(9)	0.0505	0.0502(3)
O3	0.4174	0.415(3)	0.0930	0.093(1)	0.1683	0.1685(2)
O4	0.7513	0.751(2)	0.3110	0.310(2)	0.1575	0.1576(3)
O5	0.2522	0.250(2)	0.3705	0.371(1)	0.1689	0.1685(3)
5						
K	0	0	0.0982	0.099(1)	0.25	0.25
M	0.2511	0.2496(7)	0.0836	0.0833(2)	0.0001	0.0000(1)
T1	0.9648	0.9642(8)	0.4294	0.431(1)	0.1356	0.1353(2)
T2	0.4517	0.451(1)	0.2584	0.259(1)	0.1354	0.1353(2)
O1	0.4579	0.461(2)	-0.0562	-0.056(1)	0.0536	0.0534(3)
O2	0.3858	0.385(2)	0.2528	0.2513(4)	0.0537	0.0534(2)
OH	0.4565	0.457(1)	0.5636	0.5619(9)	0.0503	0.0503(3)
O3	0.4170	0.420(3)	0.0926	0.094(1)	0.1683	0.1683(2)
O4	0.7510	0.747(2)	0.3112	0.314(2)	0.1582	0.1577(3)
O5	0.2510	0.247(2)	0.3705	0.369(1)	0.1690	0.1683(3)
6						
K	0	0	0.0988	0.099(1)	0.25	0.25
M	0.2499	0.2499(7)	0.0834	0.0833(2)	0.0000	0.0000(1)
T1	0.9649	0.9643(8)	0.4297	0.430(1)	0.1358	0.1357(2)
T2	0.4515	0.451(1)	0.2586	0.259(1)	0.1358	0.1357(2)
O1	0.4612	0.461(2)	-0.0564	-0.057(1)	0.0536	0.0535(3)
O2	0.3853	0.385(2)	0.2518	0.2514(4)	0.0536	0.0535(2)
OH	0.4567	0.457(1)	0.5626	0.5618(9)	0.0505	0.0504(3)
O3	0.4165	0.418(3)	0.0931	0.093(1)	0.1688	0.1687(2)
O4	0.7510	0.749(2)	0.3106	0.312(2)	0.1582	0.1579(3)
O5	0.2504	0.248(3)	0.3707	0.370(1)	0.1694	0.1687(3)
7						
K	0	0	0.0979	0.099(1)	0.25	0.25
M	0.2498	0.2503(7)	0.0833	0.0835(2)	0.0000	0.0000(1)
T1	0.9645	0.9646(8)	0.4295	0.430(1)	0.1364	0.1365(2)
T2	0.4508	0.451(1)	0.2584	0.258(1)	0.1364	0.1365(2)
O1	0.4620	0.460(2)	-0.0558	-0.057(1)	0.0538	0.0538(3)
O2	0.3842	0.386(2)	0.2518	0.2515(4)	0.054	0.0538(2)
OH	0.4571	0.456(1)	0.5622	0.5623(9)	0.0508	0.0504(3)
O3	0.4108	0.411(3)	0.0928	0.093(1)	0.1695	0.1698(2)
O4	0.7524	0.752(2)	0.3077	0.308(2)	0.1585	0.1585(3)
O5	0.2518	0.252(2)	0.3727	0.373(1)	0.1700	0.1698(3)
8						
K	0	0	0.0985	0.099(1)	0.25	0.25
M	0.2487	0.2498(7)	0.0829	0.0833(2)	0.0000	0.0000(1)
T1	0.9651	0.9644(8)	0.4296	0.430(1)	0.1355	0.1356(2)

Continued on next page

APPENDIX TABLE 1.—CONTINUED

	x		y		z			x		y		z	
	obs	mod	obs	mod	obs	mod		obs	mod	obs	mod	obs	mod
T2	0.4517	0.450(1)	0.2584	0.259(1)	0.1355	0.1356(2)	O3	0.4170	0.417(3)	0.0935	0.093(1)	0.1684	0.1690(2)
O1	0.4613	0.461(2)	-0.0564	-0.057(1)	0.0535	0.0535(3)	O4	0.7502	0.751(2)	0.3103	0.310(1)	0.1578	0.1582(3)
O2	0.3846	0.385(2)	0.2517	0.2513(4)	0.0535	0.0535(2)	O5	0.2495	0.250(2)	0.3700	0.370(1)	0.1691	0.1690(3)
OH	0.4577	0.457(1)	0.5618	0.5621(9)	0.0503	0.0503(3)	15						
O3	0.4193	0.417(3)	0.0931	0.093(1)	0.1683	0.1686(2)	K	0	0	0.0962	0.097(1)	0.25	0.25
O4	0.7490	0.749(2)	0.3121	0.312(2)	0.1579	0.1577(3)	M	0.2497	0.2488(7)	0.0832	0.0831(2)	0.0000	0.0000(1)
O5	0.2489	0.248(2)	0.3692	0.370(1)	0.1689	0.1686(3)	T1	0.9642	0.9626(8)	0.4286	0.431(1)	0.1354	0.1355(2)
			9				T2	0.4527	0.451(1)	0.2578	0.260(1)	0.1354	0.1355(2)
K	0	0	0.099	0.099(1)	0.25	0.25	O1	0.4572	0.460(2)	-0.0602	-0.058(1)	0.0538	0.0540(3)
M	0.2498	0.2498(7)	0.0833	0.0833(2)	0.0000	0.0000(1)	O2	0.3924	0.388(2)	0.2514	0.2511(4)	0.0537	0.0540(2)
T1	0.9653	0.9656(8)	0.4297	0.430(1)	0.1353	0.1353(2)	OH	0.4549	0.456(1)	0.5646	0.5628(9)	0.0510	0.0511(3)
T2	0.4514	0.452(1)	0.2585	0.259(1)	0.1353	0.1353(2)	O3	0.4344	0.440(3)	0.0927	0.095(1)	0.1682	0.1685(2)
O1	0.4614	0.461(2)	-0.0560	-0.057(1)	0.0533	0.0533(3)	O4	0.7402	0.737(2)	0.3211	0.325(2)	0.1597	0.1597(3)
O2	0.3838	0.385(2)	0.2514	0.2514(4)	0.0533	0.0533(2)	O5	0.2410	0.235(2)	0.3611	0.359(1)	0.1687	0.1685(3)
OH	0.4574	0.457(1)	0.5617	0.5621(9)	0.0502	0.0502(3)	16						
O3	0.4168	0.416(3)	0.0933	0.093(1)	0.1682	0.1683(2)	K	0	0	0.0932	0.097(1)	0.25	0.25
O4	0.7513	0.751(2)	0.3109	0.310(2)	0.1572	0.1573(3)	M	0.2471	0.2483(7)	0.0827	0.0830(2)	-0.0007	0.0000(1)
O5	0.2511	0.251(2)	0.3705	0.371(1)	0.1687	0.1683(3)	T1	0.9649	0.9638(8)	0.4299	0.430(1)	0.1351	0.1352(2)
			10				T2	0.4543	0.452(1)	0.2581	0.259(1)	0.1366	0.1359(2)
K	0	0	0.0986	0.099(1)	0.25	0.25	O1	0.4578	0.460(2)	-0.0574	-0.058(1)	0.0530	0.0539(3)
M	0.2499	0.2498(7)	0.0831	0.0833(2)	0.0000	0.0000(1)	O2	0.3917	0.388(2)	0.2519	0.2510(4)	0.0540	0.0539(2)
T1	0.9648	0.9650(8)	0.4300	0.431(1)	0.1354	0.1355(2)	OH	0.4604	0.456(1)	0.5645	0.5632(9)	0.0511	0.0514(3)
T2	0.4517	0.451(1)	0.2588	0.259(1)	0.1355	0.1355(2)	O3	0.4310	0.433(3)	0.0931	0.094(1)	0.1680	0.1688(2)
O1	0.4610	0.462(2)	-0.0568	-0.056(1)	0.0534	0.0534(3)	O4	0.7415	0.742(2)	0.3180	0.320(2)	0.1599	0.1595(3)
O2	0.3841	0.384(2)	0.2513	0.2514(4)	0.0534	0.0534(2)	O5	0.2406	0.240(2)	0.3623	0.363(1)	0.1692	0.1688(3)
OH	0.4557	0.457(1)	0.5620	0.5620(9)	0.0501	0.0502(3)	17						
O3	0.4171	0.418(3)	0.0935	0.093(1)	0.1681	0.1684(2)	K	0	0	0.0964	0.095(1)	0.25	0.25
O4	0.7499	0.750(2)	0.3109	0.311(2)	0.1574	0.1576(3)	M	0.2486	0.2481(7)	0.0829	0.0826(2)	0.0000	0.0000(1)
O5	0.2485	0.250(2)	0.3701	0.371(1)	0.1686	0.1684(3)	T1	0.9643	0.9650(8)	0.4293	0.428(1)	0.1356	0.1360(2)
			11				T2	0.4522	0.453(1)	0.2586	0.258(1)	0.1356	0.1360(2)
K	0	0	0.0979	0.098(1)	0.25	0.25	O1	0.4582	0.459(2)	-0.0598	-0.060(1)	0.0541	0.0541(3)
M	0.2507	0.2500(7)	0.0835	0.0834(2)	-0.0001	0.0000(1)	O2	0.3916	0.391(2)	0.2516	0.2509(4)	0.0541	0.0541(2)
T1	0.9647	0.9632(8)	0.4289	0.430(1)	0.1357	0.1357(2)	OH	0.4556	0.456(1)	0.5643	0.5643(9)	0.0519	0.0520(3)
T2	0.4520	0.450(1)	0.2578	0.259(1)	0.1356	0.1357(2)	O3	0.4335	0.431(3)	0.0933	0.092(1)	0.1689	0.1690(2)
O1	0.4620	0.460(2)	-0.0579	-0.057(1)	0.0536	0.0537(3)	O4	0.7410	0.744(2)	0.3206	0.318(2)	0.1598	0.1602(3)
O2	0.3903	0.386(2)	0.2516	0.2514(4)	0.0537	0.0537(2)	O5	0.2410	0.244(2)	0.3621	0.363(1)	0.1691	0.1690(3)
OH	0.4555	0.457(1)	0.5636	0.5624(9)	0.0504	0.0505(3)	18						
O3	0.423	0.422(3)	0.0929	0.094(1)	0.1684	0.1684(3)	K	0	0	0.0963	0.096(1)	0.25	0.25
O4	0.7472	0.746(2)	0.3137	0.315(2)	0.1584	0.1584(3)	M	0.2472	0.2479(7)	0.0825	0.0826(2)	0.0000	0.0000(1)
O5	0.2437	0.245(2)	0.3674	0.368(1)	0.1692	0.1684(3)	T1	0.9638	0.9639(8)	0.4293	0.429(1)	0.1355	0.1358(2)
			12				T2	0.4520	0.452(1)	0.2586	0.258(1)	0.1355	0.1358(2)
K	0	0	0.0988	0.099(1)	0.25	0.25	O1	0.4576	0.459(2)	-0.0607	-0.060(1)	0.0540	0.0541(3)
M	0.25	0.2504(7)	0.0836	0.0835(2)	0.0000	0.0000(1)	O2	0.3928	0.391(2)	0.2515	0.2509(4)	0.0540	0.0541(2)
T1	0.9649	0.9653(8)	0.4301	0.430(1)	0.1355	0.1357(2)	OH	0.4559	0.456(1)	0.5641	0.5636(9)	0.0522	0.0520(3)
T2	0.4511	0.451(1)	0.2586	0.259(1)	0.1355	0.1357(2)	O3	0.4416	0.438(3)	0.0933	0.093(1)	0.1688	0.1692(2)
O1	0.4618	0.461(2)	-0.0566	-0.057(1)	0.0538	0.0535(3)	O4	0.7363	0.739(2)	0.3251	0.323(2)	0.1605	0.1604(3)
O2	0.3864	0.385(2)	0.2510	0.2515(4)	0.0537	0.0535(2)	O5	0.2362	0.238(2)	0.3579	0.359(1)	0.1693	0.1692(3)
OH	0.4576	0.457(1)	0.5622	0.5625(9)	0.0502	0.0502(3)	19						
O3	0.4184	0.410(3)	0.0936	0.093(1)	0.1684	0.1688(2)	K	0	0	0.0956	0.095(1)	0.25	0.25
O4	0.7512	0.754(2)	0.3110	0.307(2)	0.1578	0.1577(3)	M	0.2466	0.2471(7)	0.0823	0.0823(2)	0.0000	0.0000(1)
O5	0.2506	0.254(2)	0.3703	0.374(1)	0.1690	0.1688(3)	T1	0.9635	0.9644(8)	0.429	0.428(1)	0.1355	0.1355(2)
			13				T2	0.4522	0.454(1)	0.2586	0.257(1)	0.1355	0.1355(2)
K	0	0	0.0985	0.097(1)	0.25	0.25	O1	0.4567	0.458(2)	-0.0614	-0.061(1)	0.0541	0.0542(3)
M	0.2491	0.2492(7)	0.0831	0.0830(2)	0.0000	0.0000(1)	O2	0.3946	0.393(2)	0.2515	0.2507(4)	0.0541	0.0542(2)
T1	0.9659	0.9645(8)	0.4297	0.430(1)	0.1354	0.1353(2)	OH	0.4557	0.456(1)	0.5646	0.5642(9)	0.0527	0.0525(3)
T2	0.4514	0.452(1)	0.2584	0.258(1)	0.1355	0.1353(2)	O3	0.4469	0.443(3)	0.0934	0.092(1)	0.1689	0.1690(3)
O1	0.4612	0.459(2)	-0.0562	-0.059(1)	0.0534	0.0537(3)	O4	0.7333	0.736(2)	0.3279	0.325(2)	0.1610	0.1609(2)
O2	0.3844	0.389(2)	0.2518	0.2512(4)	0.0536	0.0537(2)	O5	0.2329	0.236(2)	0.3552	0.356(1)	0.1693	0.1690(2)
OH	0.4570	0.456(1)	0.5619	0.5632(9)	0.0504	0.0509(3)	20						
O3	0.4190	0.424(3)	0.0933	0.093(1)	0.1684	0.1683(2)	K	0	0	0.0936	0.092(1)	0.25	0.25
O4	0.7491	0.747(2)	0.3116	0.314(2)	0.1578	0.1585(3)	M	0.2463	0.2459(7)	0.0815	0.0815(2)	-0.0001	0.0000(1)
O5	0.2487	0.246(2)	0.3696	0.367(1)	0.1690	0.1683(3)	T1	0.9619	0.9635(8)	0.4281	0.425(1)	0.1352	0.1352(2)
			14				T2	0.4524	0.455(1)	0.2580	0.255(1)	0.1352	0.1352(2)
K	0	0	0.0982	0.098(1)	0.25	0.25	O1	0.4530	0.453(2)	-0.0651	-0.067(1)	0.0549	0.0547(3)
M	0.2496	0.2495(7)	0.0833	0.0832(2)	0.0000	0.0000(1)	O2	0.4016	0.401(2)	0.2513	0.2504(4)	0.0546	0.0547(2)
T1	0.9649	0.9659(8)	0.4296	0.429(1)	0.1355	0.1359(2)	OH	0.4555	0.454(1)	0.5651	0.5664(9)	0.0546	0.0541(3)
T2	0.4513	0.452(1)	0.2586	0.258(1)	0.1356	0.1359(2)	O3	0.4601	0.46(3)	0.0931	0.090(1)	0.1689	0.1695(2)
O1	0.4622	0.460(2)	-0.0557	-0.058(1)	0.0536	0.0537(3)	O4	0.7253	0.728(2)	0.3349	0.332(2)	0.1626	0.1628(3)
O2	0.3851	0.388(2)	0.2519	0.2513(4)	0.0535	0.0537(2)	O5	0.2256	0.228(2)	0.3478	0.346(1)	0.1692	0.1695(3)
OH	0.4569	0.456(1)	0.5617	0.5628(9)	0.0502	0.0506(3)							

Supplemental Discussion to

“Structural regularities in $2M_1$ dioctahedral micas: the structure modeling approach”

by Bella B. Zviagina and Victor A. Drits.

In the initial review of the manuscript “Structural regularities in $2M_1$ dioctahedral micas: the structure modeling approach” a question was raised as to how the various ways of predicting mean octahedral and tetrahedral bond lengths, $d(\text{M-O,OH})$ and d_T , suggested by previous authors compare with Equations 1 and 7 obtained in the present work. A comprehensive discussion on this issue is beyond the scope of the primary paper and is therefore dealt with in the following Supplemental Discussion.

Mean octahedral bond lengths

The coefficients d_i for the equation $d(\text{M-O,OH}) = \sum_i c_i d_i$ suggested by Baur (1981), Weiss et al. (1992), Smoliar-Zviagina (1993), Mercier et al. (2006), and the present authors are listed in Supplement Table 1.

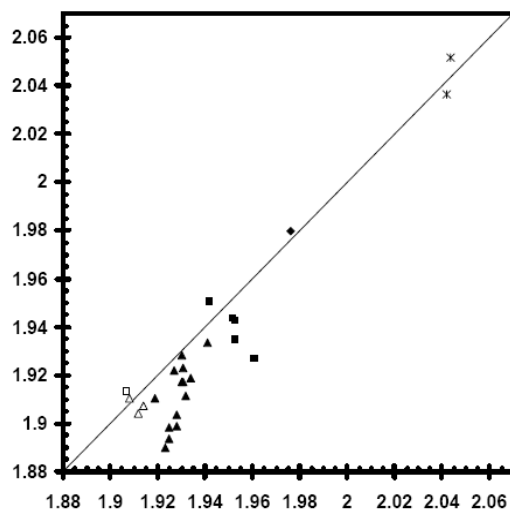
Supplementary Table 1. Coefficients d_i for the equation $d(\text{M-O,OH}) = \sum_i c_i d_i$

Cation	Baur (1981)	Weiss et al. (1992)	Smoliar-Zviagina (1993)	Mercier et al. (2006)	This work
Al	1.909	1.919	$0.816+0.214b^*$	1.945	1.918
Mg	2.085	2.083	2.060	2.076	2.065
Fe ²⁺	2.136	2.11	2.120	2.126	2.063
Fe ³⁺	2.011	2.053	1.980	2.026	2.028
Ti	-	2.073	1.945	-	1.900
Cr	1.999	2.04	1.950	-	2.000
Mn ²⁺	-	2.14	-	-	2.200
Mn ³⁺	-	-	1.980	-	2.000

* b = unit-cell parameter

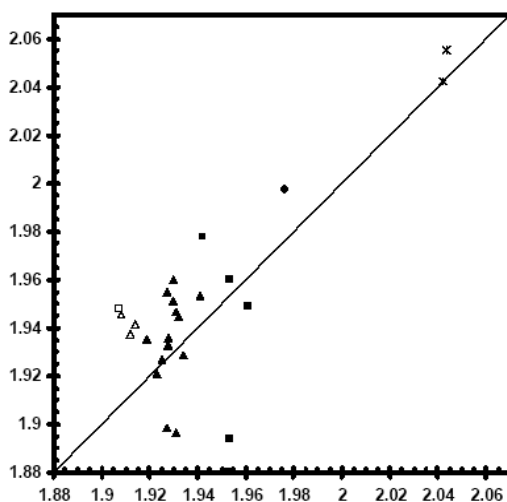
The d_i values of Drits (1969, 1975) are not given, as they were generalized in the equation of Smoliar-Zviagina (1993).

Supplement Figure 1, where the mean octahedral bond lengths calculated using the d_i values of Baur (1981) are plotted against the observed mean octahedral bond lengths in refined dioctahedral mica structures, shows that the predicted $d(\text{M-O,OH})$ values are severely underestimated (on average, by 0.015 Å), with reasonable agreement only for paragonites and margarites.



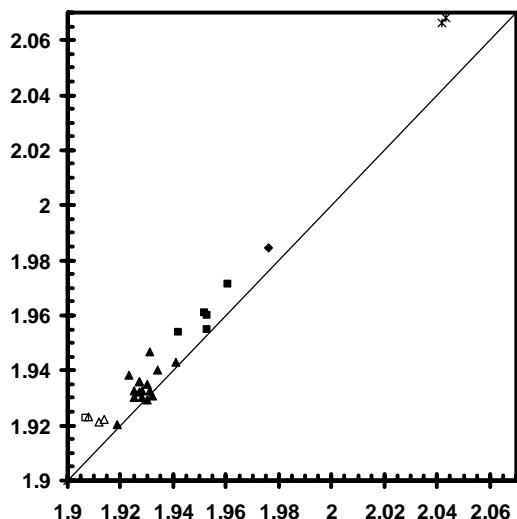
Supplement Figure 1. Comparison of predicted (Baur, 1981) and observed mean octahedral bond lengths $d(\text{M-O,OH})$ in dioctahedral micas. Symbols: black triangle = muscovite-2M₁, black square = Fe- and/or Mg-rich muscovite and phengite-2M₁, diamond = aluminoceladonite-2M₁, open triangle = paragonite-2M₁, open square = margarite-2M₁, asterisk =

The $d(\text{M-O,OH})$ values calculated according to Mercier et al. (2006) (Supplement Figure 2) show a wide scatter of points, with $\text{esd}=0.03$ Å and the discrepancies between the calculated and observed values up to 0.04 Å.



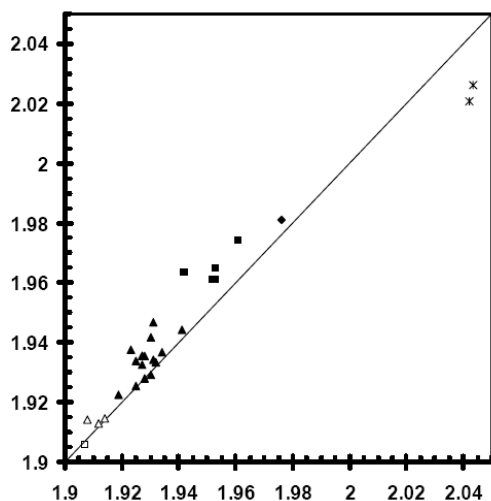
Supplement Figure 2. Comparison of predicted (Mercier et al., 2006) and observed $d(\text{M-O,OH})$ values in dioctahedral micas (symbols as in Supplement Figure 1).

The approach of Weiss et al. (1992) provides better agreement between the predicted and observed $d(\text{M-O,OH})$ values, although the latter are systematically overestimated, on average, by 0.008 Å (Supplement Figure 3).



Supplement Figure 3. Comparison of predicted (Weiss et al., 1992) and observed $d(\text{M-O,OH})$ values in dioctahedral micas (symbols as in Supplement Figure 1).

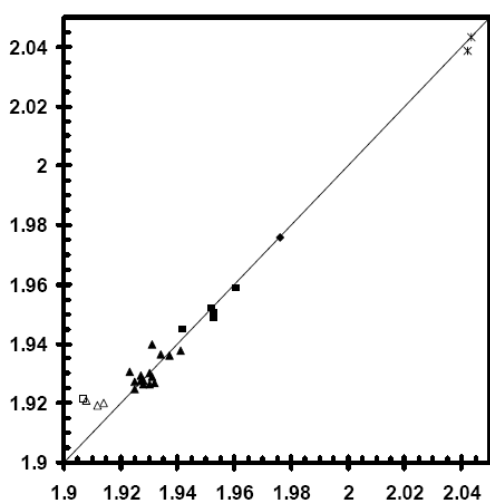
The equation of Smoliar-Zviagina (1993) overestimates the $d(\text{M-O,OH})$ values for dioctahedral micas- $2M_1$ by, on average, 0.005 Å, and underestimates those for celadonites- $1M$ by about 0.02 Å (Supplement Figure 4).



Supplement Figure 4. Comparison of predicted (Smoliar-Zviagina, 1993) and observed $d(\text{M-O,OH})$ values in dioctahedral micas (symbols as in Supplement Figure 1).

The equation obtained in the present work (Eq. 1) describes the $d(\text{M-O,OH})$ values in K-dioctahedral micas with $\text{esd} = 0.003 \text{ \AA}$, $r^2 = 0.983$, $p\text{-value} < 10^{-10}$, whereas those for paragonites and margarite are overestimated by 0.006-0.014 Å, so that the overall esd and r^2 are 0.005 Å and 0.979, respectively (Supplement Figure 5). The best agreement between the calculated and observed mean octahedral bond lengths in K-dioctahedral micas is therefore provided by

Equation 1 of the present work, whereas the $d(\text{M-O,OH})$ in paragonites and margarites are best described using either the approach of Smoliar-Zviagina (1993) or that of Baur (1981).



Supplement Figure 5. Comparison of predicted (this work) and observed $d(\text{M-O,OH})$ values in dioctahedral micas (symbols as in Supplement Figure 1).

Mean tetrahedral bond lengths

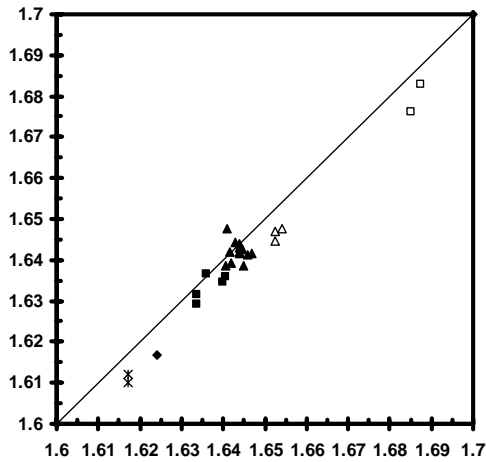
The equations for predicting mean tetrahedral bond lengths suggested in different works including the present study are given in Supplement Table 2.

Supplement Table 2. Equations for predicting mean tetrahedral bond lengths (Si and Al^{IV} are amounts of Si and Al cations in tetrahedra (phfu)).

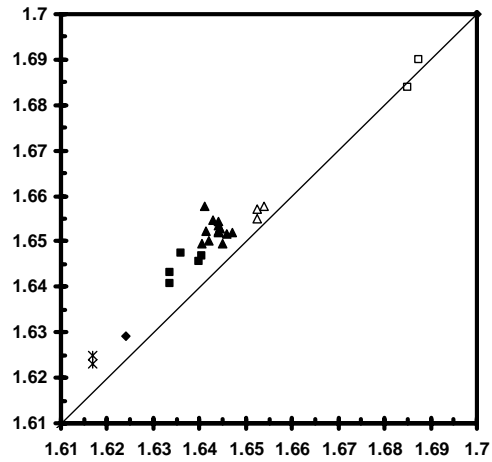
Reference	Equation
Drits (1975)	$d_T = 1.61(\text{Si}/4) + 1.75(\text{IV Al}/4)$
Baur (1981)	$d_T = 1.623(\text{Si}/4) + 1.752(\text{IV Al}/4)$
Hazen and Burnham (1973)	$d_T = 1.608 + 0.163(\text{IV Al}/4)$
Brigatti and Guggenheim (2002)	$d_T = 1.607 + 0.042 \text{IV Al} =$ $1.607 + 0.168(\text{IV Al}/4)$
Mercier et al. (2006)	$d_T = 1.610(\text{Si}/4) + 1.787(\text{IV Al}/4)$
Smoliar-Zviagina (1993)	$d_T = 1.616 + 0.160(\text{IV Al}/4)^{1.25}$
This work	$d_T = 1.6192 + 0.1569(\text{IV Al}/4)^{1.25}$

The d_T values calculated using the approach of Drits (1975) are systematically underestimated, the average discrepancy between the calculated and observed values being -

0.003 Å, reaching -0.007 to -0.009 Å in the case of aluminoceladonite- $2M_1$ and celadonites- $1M$ (Supplement Figure 6).



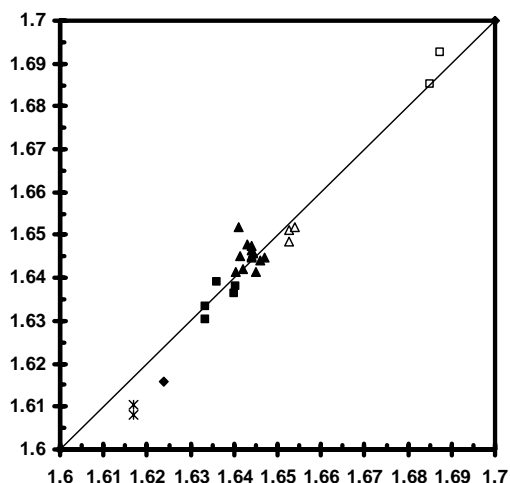
Supplement Figure 6. Comparison of predicted (Drita, 1975) and observed d_T values in dioctahedral micas (symbols as in Supplement Figure 1).



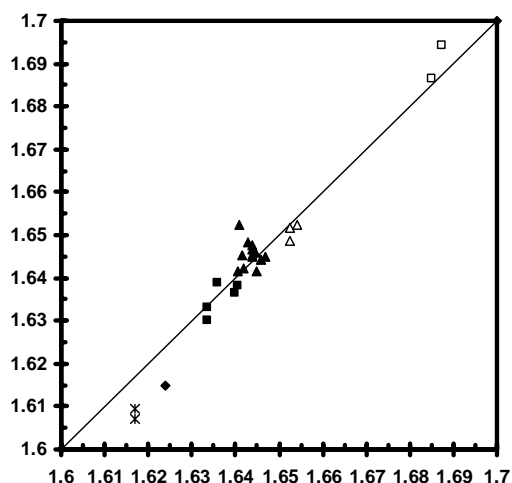
Supplement Figure 7. Comparison of predicted (Baur, 1981) and observed d_T values in dioctahedral micas (symbols as in Supplement Figure 1).

The equation of Baur (1981) provides close agreement between predicted and observed d_T values for paragonites and margarites, whereas the predicted d_T in K-dioctahedral micas are systematically overestimated, on average, by 0.007 Å (Supplement Figure 7).

The equations of Hazen and Burnham (1973) and Brigatti and Guggenheim (2002) are very similar (Supplement Table 2) and therefore lead to virtually identical results (Supplement Figures 8 and 9): good agreement between calculated and observed d_T (esd = 0.004 Å and 0.005 Å, respectively; $r^2 = 0.95$), with the d_T in micas having low tetrahedral Al contents (aluminoceladonite- $2M_1$ and celadonites- $1M$) underestimated by 0.007-0.010 Å.

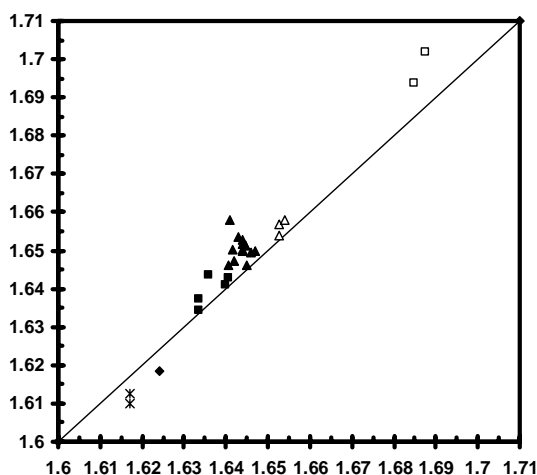


Supplement Figure 8. Comparison of predicted (Hazen and Burnham, 1973) and observed d_T values in dioctahedral micas (symbols as in Supplement Figure 1).



Supplement Figure 9. Comparison of predicted (Brigatti and Guggenheim, 2002) and observed d_T values in dioctahedral micas (symbols as in Supplement Figure 1).

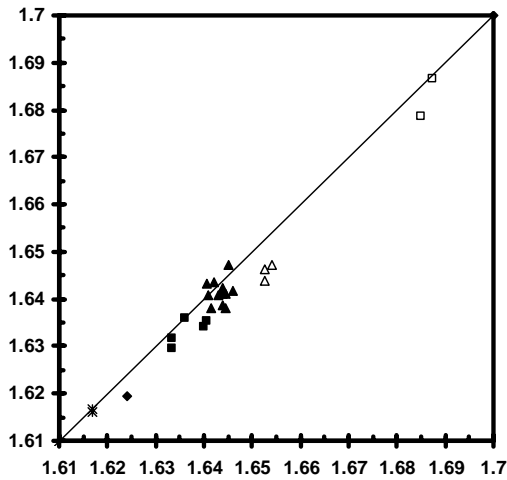
The d_T values calculated using the equation of Mercier et al. (2006) are systematically overestimated (on average, by 0.006 Å, with discrepancies up to 0.017 Å) for all the samples except aluminoceladonite- $2M_1$ and celadonites $1M$, where the d_T are underestimated by up to 0.007 Å (Supplement Figure 10)



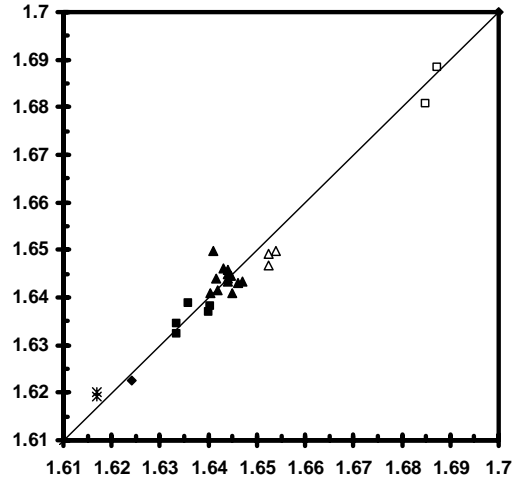
Supplement Figure 10. Comparison of predicted (Mercier et al., 2006) and observed d_T values in dioctahedral micas (symbols as in Supplement Figure 1).

The equation of Smoliar-Zviagina (1993) was only slightly modified in the present work to account for contemporary high-precision refined structural data (Supplement Table 2). The two regressions provide similar results (esd = 0.003 Å, $r^2 = 0.958$, p-value $< 10^{-10}$ in both cases) but

that of Smoliar-Zviagina (1993) tends to systematically underestimate the d_T values (on average, by 0.003 Å) (Supplement Figures 11 and 12).



Supplement Figure 11. Comparison of predicted (Smoliar-Zviagina, 1993) and observed d_T values in dioctahedral micas (symbols as in Supplement Figure 1).



Supplement Figure 12. Comparison of predicted (this work) and observed d_T values in dioctahedral micas (symbols as in Supplement Figure 1).

To summarize, Equation 7 of the present work shows the best statistical parameters and describes equally well the d_T at both high and low tetrahedral Al contents, although the regression of Hazen and Burnham (1973)/ Brigatti and Guggenheim (2002) is of comparable predictive quality and provides slightly better agreement between the calculated and observed d_T values in paragonites.

References to Supplemental Discussion

- Baur, W.H. (1981) Interatomic distance prediction for computer simulation of crystal structures. In M. O'Keefe and A. Navrotsky, Eds., *Structure and Bonding in Crystals*, p. 31–52. Academic Press, New York.
- Brigatti, M.F. and Guggenheim, S. (2002) Mica crystal chemistry and the influence of pressure, temperature and solid solution on atomistic models. In A. Mottana, F.E. Sassi, J.B. Thompson Jr., and S. Guggenheim, Eds., *Micas: Crystal chemistry and metamorphic petrology*, 46, p.

- 1–97. Reviews in Mineralogy and Geochemistry, Mineralogical Society of America, Chantilly, Virginia, with Accademia Nazionale dei lincei, Roma, Italy.
- Drits, V.A. (1969) Some remarks on the structure of trioctahedral micas. Proceedings of the 4th International Clay Conference, Tokyo, 1, 51-59.
- Drits, V.A. (1975) Structural and crystal-chemical features of layer silicates. In A.G. Kossovskaya, Ed., *Kristallokhimiya mineralov i geologicheskiye problemy*, p. 35-51. Nauka, Moscow (in Russian).
- Hazen, R.M. and Burnham, C.W. (1973) The crystal structures of one-layer phlogopite and annite. *American Mineralogist*, 58, 889-900.
- Mercier, P.H.J., Rancourt, D.G., Redhammer, G.J., Lalonde, A.E., Robert, J.-L., Berman, R.G., and Kodama, H. (2006) Upper limit of the tetrahedral rotation angle and factors affecting octahedral flattening in synthetic and natural *1M* polytype *C2/m* space group micas. *American Mineralogist*, 91, 831-849.
- Smoliar-Zviagina, B.B. (1993) Relationships between structural parameters and chemical composition of micas. *Clay Minerals*, 25, 603-624.
- Weiss, Z., Rieder, M., and Chmielova, M. (1992) Deformation of coordination polyhedra and their sheets in phyllosilicates. *European Journal of Mineralogy*, 4, 665-682.